ADDIS ABABA UNIVERSITY

ADDIS ABABA INSTITUTE OF TECHNOLOGY

SCHOOL OF MULTI-DISCIPLINARY ENGINEERING

CENTER FOR MATERIALS ENGINEERING

Synthesis and characterization of Cellulose-based Aerogel from Mixed Organic Solid Wastes

A Thesis Submitted to the Center for Materials Engineering, Addis Ababa Institute of Technology, in Partial Fulfilment of the Requirements for the Degree of Masters in Materials Engineering

By Kidist Worku

October, 2020

Addis Ababa, Ethiopia

ADDIS ABABA INSTITUTE OF TECHNOLOGY
SCHOOL OF MULTIDISIPLINARY ENGINEERING
CENTER FOR MATERIALS ENGINEERING

Synthesis and characterization of Cellulose-based Aerogel from Mixed Organic Solid Wastes

By Kidist Worku

Approved By the Examining Board	Signatures	Date
Dr. Sintayehu Nibret (Chair, Department Graduate Committee)	_____	_____
Dr. Dawit Ayana (Advisor)	_____	_____
Dr. Tesfaye Refera (Internal Examiner)	_____	_____
Dr. Shimelis Kebede (External Examiner)	_____	_____

DECLARATION

I Kidist Worku registration number GSR/0104/2011, do hereby declare that this thesis is my original work and that it has not been previously submitted partially or in full, by any other person for an award of degree in any other university/institution. All resources of materials used in this document have all been duly acknowledged.

Submitted by:

Full Name: Kidist Worku Signature: _____ Date: _____

Approved by:

This thesis has been submitted for examination with my approval as University Advisor

Name of Advisor: Dr. Dawit Gemechu Signature_____Date_____

Table of Contents

List of Figures

List of Tables

List of Acronyms

BET	Brunauer-Emmet-Teller
BP	Banana peel
CBA	Cellulose-based aerogel
FE-SEM	Field Emission Scanning electron microscopy
FTIR	Fourier transfer infrared spectroscopy
HTSCD	High temperature supercritical drying
LTSCD	Low temperature supercritical drying
Rt	Ratio and time
SSA_{BET}	Specific surface area
UV/Vis	Ultraviolet/Visible Light spectroscopy
WCF	Waste cotton fabric
WP	Waste paper

Acknowledgement

First and foremost, praises and thanks be to God Almighty, for his blessings throughout my research work. I would like to express my deep and sincere gratitude to my research advisor, Dr. Dawit Gemechu, for his continuous and consistent supervision and consultation on my research work. His commitment, patience, enthusiasm, motivation and guidance helped me through the research and writing of the thesis. I would like to thank Dr. Sintayehu Nibret, Head of Center for Materials Engineering, for his comments and cooperation in the process of accessing available laboratory facilities. I also would like to thank all laboratory assistants at Chemical Engineering laboratory of AAiT and Addis Ababa Science & Technology University. I also would like to extend my appreciation to Dr. Yonas Chebude at chemistry department of AAU, College of Natural Science, for helping me freeze dry my samples at the chemistry department laboratory in spite of the lockdown due to covid-19 pandemic.

Abstract

Cellulose-based aerogels are materials that are produced from cellulose, which is the most abundantly available natural polymer. Like other aerogels, cellulose-based aerogels have low density and highly porous structure made from interconnected network of cellulose fibers. Those properties of cellulose-based aerogels prepared from easily available raw materials, that make it potential alternative material applicable for the removal of oil and organic solvents. The direct discharge of oil and organic solvent containing waste water damages the marine ecological environment and intoxicate life thereby, imposing immediate and longtime damages. In this work, cellulose-based aerogels were synthesized by mixing cellulose-rich organic solid waste materials. Cellulose-based aerogels were produced combining textile cotton fabric (100 % cotton), waste paper, and waste banana peel without pretreatment. Sol-gel process followed by freeze drying was executed to successfully fabricate the cellulose-based aerogel. Precooled NaOH/urea solution was used at standard NaOH/Urea/water (7:12:81) ratio for cellulose dissolution by varying precursor/solvent ratio and dissolution time. Further, hydrophobic modification using carbon nanoparticles/acetone solution was performed to the cellulose-based aerogel with the best characteristic properties. This gave the aerogel an oil/organic solvent selectivity property during waste water treatment. A cellulose-based aerogel with the lowest density of 0.127 g/cm^3 that showed a macroporous structure with 91.5 % porosity and specific surface area of 192.24 m^2/g. Sorption capacity and removal efficiency tests were done for cooking oil, engine/motor oil, ethanol, and benzene. Accordingly, sorption capacities of 15.74, 13.81, 13.98, and 13.98 g/g were recorded respectively. After the removal tests the efficiency of cellulose-based aerogels were found to be 80.89 % for cooking oil, 77.2 % for engine/motor oil, 76.48 % for ethanol, and 74.1 % for benzene. The aerogel was recycled to be reused a number of times in which it was able to remove more than 50 % of contaminants up to the third cycle. Hence, the characteristics and pollutant removal performance of cellulose-based aerogel make it a potential candidate for oily and organic solvent containing waste water treatment.

Key words: Cellulose-based Aerogels, Sol-gel Method, NaOH/Urea Solvent, Freeze Drying, Oil and organic solvent removal

Chapter I

1.1 Introduction

Aerogel materials are highly porous materials with very low densities and a high specific surface area (Onwukamike et al., 2019). The precursors for aerogel production are of variety of substances such as silica, transition metal oxides, and organic polymers like cellulose. Some of the commercial applications of aerogels include thermal insulation, catalysts, windows, absorbents and particle detectors. Aerogels are favoured for oil and organic solvent removal purposes because of their versatile mesoporousity, outstanding mechanical flexibility and long channel structure (Yue, Zhang, Yang, Qiu, & Li, 2018).

As the most abundant natural organic polymer, cellulose is a potential and viable replacement for the unsustainable fossil based polymers being used today (Dieter Klemm, Heublein, Fink, & Bohn, 2005). It has recently been popularly used as aerogel precursor. Cellulose-based aerogels can be modified into highly hydrophobic and super oleophilic which enables them to selectively absorb oils and other organic liquids from water surface with high sorption capacities (Yue et al., 2018).

Aerogels are generally prepared using sol-gel processing procedures followed by additional procedures to enhance mechanical properties and characteristics of the gel (Dorcheh & Abbasi, 2008). All steps involved in synthesis contribute to the framework of the gel and influence its properties and thus corresponding applications. In cellulose-based aerogel (CBA) processing, direct processing is not possible because cellulose has no thermal transition or melting point. However, cellulose can be shaped into various forms through solubilization and subsequent regeneration using selected solvents.(Dieter Klemm et al., 2005).

According to the Addis Ababa sanitation, beautification and park development agency, the solid waste generated from the city is assumed 76 % from household, 18 % from institution and 6 % from street sweeping (Amera, 2010). This indicates that the waste is mainly organic waste and potentially sustainable resource for cellulose. Among the constituents of municipal solid waste are waste paper, banana peel and textile fabrics which are sources of high cellulose contents around, 85 %, 18 %, and 90% respectively (Nguyen et al., 2013), (Romelle, Rani, & Manohar, 2016), (Dieter Klemm et al., 2005).

Several biomass materials have been used as precursors to prepare aerogels so far, and interesting properties have been recorded. Among those biomasses are waste paper, banana peel and textile fabric. Previously done researches such as(Jin, Han, Li, & Sun, 2015), show that hydrophobic CBA aerogels

prepared from waste newspaper with high absorption of oil contaminant and high density solvents from water surface. These results can be influenced by the CBA properties such as high selectivity of contaminant and porosity. Banana peel (BP) is rich in pectin, lignin, hemicelluloses and proteins, along with cellulose that make it viable precursor of carbon-based aerogel via simple freezing-cast process (Padam, Tin, Chye, & Abdullah, 2014). BP-derived micro-sheet is strongly immobilized on the aerogel structure belt, which would benefit to maintain the special hierarchical structure of aerogel (Yue et al., 2018). The other cellulose rich materials is textile cotton fabric, that showed comparable values of tensile and flexural strength to that of other fibre reinforced polymer composites (He et al., 2018).

In this research, it is anticipated to combine cellulose rich waste materials waste paper (WP), banana peel (BP), and waste cotton fabrics (WCF) as precursors and prepare aerogel that can be applicable for oil and organic solvent separation purposes in waste water treatment applications. It was desired to cultivate properties from individual precursors and a composite cellulose-based aerogel that exhibit good mechanical strength, porosity, and hydrophobic/oleophilic properties simultaneously.

1.2 Problem Statement

The environmental issues raised these days are mainly the outcomes of the daily waste generated from human activities. Generated waste of any type, i.e. solid waste, waste water or air pollutants, if not well managed can cause a serious problem in degrading the quality our environment. The result of poor environmental management is manifested by the quick degradation of our environment. Climate change, global warming, lack of clean living environment i.e. clean air and clean water access, are among the major problems we are dealing with these days. Waste water discharged into environment, in particular, have posed serious problems contaminating surface and ground water.

Oil and organic solvents containing wastewater are generated from industrial technologies including the petrochemical, food, textile, leather, steel, and metal finishing industries. The direct discharge of oil and toxic organic solvent containing waste water into water bodies brings serious damages to the ecological environment(Ma et al., 2017).Oil and organic solvent containing waste water causes immediate and long-term environmental damages that last for decades. Oil spills cling to every surface they touch and become long-term parts of every ecosystem they enter. Discharged oil floats on water surfaces and hinders air and sunlight entering that interferes with natural process of marine life decreasing dissolved oxygen. Eventually oil stops floating and begins to sink into marine environment and damages fragile underwater ecosystems, contaminates, and kill fish and smaller organisms that are essential links in the global food chain(El-Gawad, 2014). Organic solvents on the other hand have toxicological properties that is highly hazardous and endangers life with extremely low biodegradability (Sanni Babu & Mutta Reddy, 2014).

In the case of Ethiopia, the major industries include food processing, textiles, beverages, chemical products, footwear, soaps, and leather among others that are potential sources of oil and organic solvent containing effluents. Specifically in the capital Addis Ababa and surroundings, where 65 % of the industries in the country locate, the rivers and water reserves are polluted by industrial and municipal solid and liquid wastes of organic and inorganic pollutants. The city generates 49 million m^3 total waste water annually, where 4 million m^3 is industrial waste water. 90 % of the industries have no kind of treatment plant that their effluents are directly discharged into the environment. The discharged effluent contaminates up stream water which then mixes with downstream shallow ground water and springs(Yohannes & Elias, 2017).

Several waste water treatment techniques have been proposed so far but high cost, low efficiency, tedious processing techniques and secondary pollution have been major difficulties (Zhang et al., 2017) Clean and sustainable waste water treatment developed utilising solid waste materials are sustainably promising

approaches in keeping the environment safe. In the case of solid waste management systems the waste stream consists of a variety of materials of large volume. The collected waste passes through a number of procedures such as incineration which consumes a large amount of energy and ultimately brought to landfilling stage where waste burial takes place. After solid waste land filling takes up a free space/land and has been completed, the area will become limited to a number of activities which is undesirable in such a time the population is growing fast and land has become an expensive commodity.

Clean water access, affordable waste water treatment techniques, and solid waste management are burning issues at the time especially for developing countries like Ethiopia. Several researches explored CBAs made from single organic solid wastes such as waste paper, textile fabrics, and corncob, separately and applied for different applications. Previous reports use processing chemicals that are expensive and of toxic nature such as ionic liquids and silane, for instance, methyltrimethoxysilan, that could create further environmental concern (Thai et al., 2020), (Nguyen et al., 2013).

In this study, cellulose based aerogels were synthesized by mixing waste cotton, waste paper and waste banana peel and the effect of dissolution time and precursor/solvent ratio were examined. The removal efficiency of CBA for oil spill clean-up and organic solvent removal from waste water were also determined.

1.3 Objective

1.3.1 General Objective

The main objective of this research is to synthesize cellulose-based aerogel from mixed easily available organic solid wastes that can be used for separation of oil and organic solvents from waste water.

1.3.2 Specific Objectives

- To prepare precursor materials for aerogel synthesis
- To synthesize cellulose-based aerogel from the selected organic solid waste materials.
- To study the effect of cellulose dissolution time and precursor/solvent ratio on the final product properties.
- To make hydrophobic modification of the CBA for a more suitable application in waste water treatment.
- To investigate characteristic properties of fabricated CBA.
- To determine the separation efficiency of the prepared CBA for oil and organic solvents removal.

1.4 Scope

The scope of this study focuses on mixing and converting cellulose rich organic solid wastes into cellulose-based aerogel. The research is limited to examining the effects of selected parameters on the characteristics of the final CBA material and its removal efficiency oil and organic solvents.

1.5 Significance of the study

The significance of this research lies on different aspects. The starting precursors are composed of cellulose-rich solid wastes taken from solid waste stream. This is advantageous since raw material is abundantly existing natural polymer found in organic solid wastes. Raw materials for this research were separated from solid waste stream and used as resources for cellulose-based aerogel fabrication. This waste to resource conversion can help to relief the load of the solid waste stream. This makes the objective and approach of this research sustainable and economical.

All the steps taken to process raw materials into CBA were low energy consuming and economical. The sodium hydroxide/urea solvent used for cellulose dissolution is environmentally less hazardous. The experiment steps including cellulose dissolution, hydrophobic modification, and freeze drying were performed at low temperatures which makes them less energy intensive processes. This makes the processing highly economical and environmentally safe.

More importantly, the target and significance of this work is to produce a cellulose-based aerogel with enhanced and combined properties contributed from individual precursors. The characteristic properties of aerogels as waste water treatment materials are discussed later in the document. Although the processing techniques have strong influence on the final product, all the three precursors contribute to the important properties like porosity, mechanical strength, and thermal stability. Ultimately the study of those properties of the aerogel helps understand its efficiency as a waste water treatment material. The CBA was used to clean up oil spills and remove organic solvents from contaminated water where significant removal was scored. In general, the study has found some significant findings in processing cellulose rich organic solid wastes into composite absorbent aerogels for waste water treatment in a cheap, sustainable, and environmentally friendly approach. These findings have significant contributions that can be used as bases for further studies in the area.

Chapter II

2. Literature Review

Aerogels are materials with the lowest weight and low densities with highly porous structures filled with gases such as air (Onwukamike et al., 2019), (Russler et al., 2012). Aerogels are prepared by forming gels from their precursors and drying the gels in a manner that maintains interconnected nanostructure that forms the porous structure of aerogels. Common wet drying techniques are freeze drying and liquid CO_2 supercritical drying which help to overcome the strong capillary forces that might cause the gel structure to collapse(Innerlohinger, Weber, & Kraft, 2006). The general aerogel process is combination of sol-gel process followed by appropriate drying technique.

Large range of materials can be used to prepare aerogels with early researches on aerogels mainly used inorganics such as silica and metal oxide (Kistler, 1931). To replace the raw materials for aerogel production with renewable materials such as cellulose have been focus of recent research interest among those cellulose-based aerogels have reported promising potential for filtration, scaffolds and drug delivery purpose (Abeer, Mohd Amin, & Martin, 2014), (Ciolacu, Rudaz, Vasilescu, & Budtova, 2016).

2.1 Cellulose-based Aerogels

The demand for a sustainable and environmentally friendly products has pressured researchers to focus their studies on a natural, renewable and degradable materials (Vargas-Jiménez, 2012). Natural nanometric cellulose fibers are considered as alternative material for various applications of biodegradable materials (Tibolla, Pelissari, & Menegalli, 2014).Cellulose is the most abundantly found natural polymer which make it sustainable/renewable replacement for the unsustainable and environmentally unsafe fossil based resources. Cellulose is a linear polysaccharide containing repeated β (1−4) linked D-glucose units. The cellulose structure has both crystalline and amorphous regions, caused by secondary interactions of polymer chains via van der Waals and hydrogen bonding. The polymer chain interactions also create parallel stacking of fibers of 5-50 nm diameter, 1 .5 g/cm^3 estimated density, 125 GPa average Young modulus, and 2.5 GPa of average tensile strength (Illera, Mesa, Gomez, & Maury, 2018). Figure 1 shows the cellulose structure containing repeated units of D-glucose units linked by β-(1,4)-glycosidic bonds that form the polysaccharide cellulose structure.

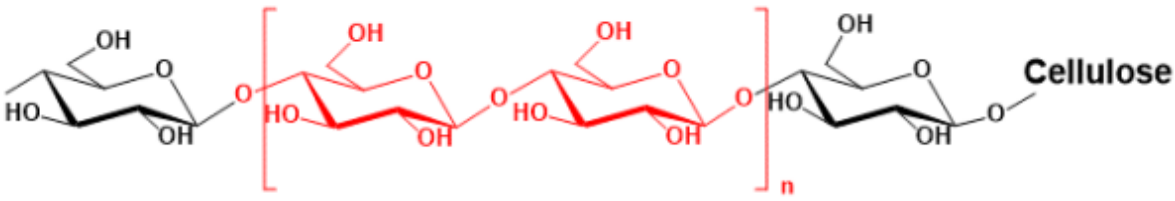

Figure 1: Cellulose chemical structure (M. O. Mohammed et al., 2017)

One of the drawbacks of cellulose is that it has no thermal transition or melting point. This property of cellulose makes it impossible to directly process it (D Klemm & Heublein, 2005). However, through solubilization and subsequent regeneration of cellulose it can be processed and shaped into various forms. Yet this approach is so challenging for cellulose is insoluble polymer in common organic solvents and also in water. The insolubility property emerges due to the inherent intra- and intermolecular hydrogen bonding in the cellulose structure (D Klemm & Heublein, 2005). Therefore solvents that can disrupt the intra and inter molecular bonds and solubilize the cellulose are required for successful solubilization of cellulose. Solvents with such capability and the factors that can affect the process such as cellulose concentration and preparation methods have been investigated so far. Those matters ultimately affect the density and volume shrinkage of the obtained aerogels(Innerlohinger et al., 2006).

2.2 Solid Waste

Studies show that waste generation rates and composition are affected by factors such as level of industrialization, climate and socio-economic development. A community of higher economic status generate solid waste composed of luxurious materials including cardboard, paper, plastic and heavier organic materials. On the other hand, the characteristics of waste generated from low income community like in developing countries are high in density and moisture content (Haile, 2016).

According to the Addis Ababa sanitation, beautification and park development agency, the sources of solid waste in Addis Ababa consist of 76 % from household, 18 % from institution and 6 % from street sweeping (A. Mohammed & Elias, 2017). An assessment that overviews the city's solid waste management shows that the solid waste is mainly of organic waste i.e. 60 % (Ababa, 2010). Although there is no study that shows the exact figure of the current composition of solid waste generated in the city, in 2010, the estimated solid waste that the city generated was 0.4 kg/capita of waste per day, with more than 200,000 metric tons annual generation. Only 65 % of the generated waste is collected while the remaining is deposited in open sites, rivers, and draining channels. The primary means of solid waste disposal in Ethiopia is to burn the garbage (Cheever, 2011).

2.2.1 Cellulose Rich Municipal Solid Wastes

Lignocellulosic biomass is the source of cellulose that is abundant and sustainable, and naturally produced resource. Cellulose is found in biomass materials entrapped with two other polymers, hemicellulose and lignin (Vargas-Aponte, 2017). Table 1 presents the composition of these three polymers in different types of biomass.

Table 1: Biomass sources and its composition (Vargas-Aponte, 2017)

Biomass	Cellulose (%)	Hemi-Cellulose (%)	Lignin (%)
Hardwood stems	40-55	24-40	18-25
Grasses	25-40	35-50	10-30
Wheat straw	30	50	15
Leaves	15-20	80-85	0
Cotton linters	80-95	5-20	0
Paper	85-99	0	0-15
Newspaper	40-55	25-4	18-30

2.2.1.1 Waste Paper

Due to the huge consumption of paper the waste paper disposed makes up 25−40 % of annual global municipal solid waste (Nguyen et al., 2013). Wastepaper is cellulosic materials where more than 85 % is cellulose and the rest is composed of lignin and other inorganic fillers such as printing inks and other process assistant materials. The cellulose rich composition of WP makes it a feasibly alternative cellulose source for cellulose-based productions (Jin et al., 2015).

Waste recycling, in this case paper recycling, gives relief to the environment alleviating or reducing waste release and environmental stressing activities such as deforestation. Recycled cellulose fibers from paper waste are a cheap and abundant resource. There are diverse pre-treatment options that help improve bioconversion efficiency of WP and cellulose dissolution. Among those processes acid/alkali treatment, steam explosion, organic solvents are common approaches (Jabbour et al., 2010).

2.2.1.2 Waste Cotton Fabric

There is continuous increment in waste generation rate mainly due to population growth and industrialization/development of countries. Textile waste particularly is affected by this and the rapid fashion cycles. Millions of tons of the fabric waste is released and managed either by disposing to landfills

or burning (Beini Zeng, Wang, & Byrne, 2019). This waste management approach has its own environmental impact. The textile materials are of different composition either synthetic polymers or natural polymers (Nunes, Godina, Matias, & Catalão, 2018), (Sandin & Peters, 2018). Natural polymers used for textile fabric production is cotton. Cotton textile fabrics are used for different applications from clothing to curtains. In 2016/17, the global cotton produced reached 23 million tone and projected to increase in years to follow (Dieter Klemm et al., 2005).

Textile fabric materials that are 100 % cotton have around 90 % cellulose composition. This cellulose content of cotton fabric make it recyclable through mechanical or chemical treatments, which make it alternative source for cellulose. Mechanical recycling is basically size reduction process which results in reduction of fiber length. The chemical treatment method lifts the recycled cotton to a 100 % cellulose. The common difficulty faced in this method is the difficulty of cotton to dissolve in common solvents which is due to the high cellulose content (Dieter Klemm et al., 2005).

Textile waste decomposition can be environmentally threatening in that decomposing clothing can release methane, a harmful greenhouse gas which is contributor to global warming. Chemicals and dyes on fabric can leach into soil to cause pollution to surface and groundwater (Thai et al., 2020). Recycled cotton waste have a characteristic mechanical tensile and flexural strength which makes it applicable for lower load bearing purposes. The recycled textile waste has lower weight which reduced its price. In some cases, natural cellulose fibres are carbon neutral by consuming more carbon dioxide than is used in cultivation (He et al., 2018).

2.2.1.3 Waste Banana Peel

Banana fruit is among the most popular fruits widely cultivated worldwide in tropical and subtropical regions, representing 40 % of the global fruit trade (Singanusong, Tochampa, Kongbangkerd, & Sodchit, 2014). Only 12 % of the fruit is edible and the rest is the peel which can be processed in various ways as food and unripe banana biomass. A significant amount of waste rich in cellulose and starch is released from banana cultivation. Therefore this makes banana peels a source of degradable materials (Elanthikkal, Gopalakrishnapanicker, Varghese, & Guthrie, 2010). Banana peel (BP) contains pectines, lignin, hemicellulose, and proteins which are soft hydrophilic organics. It is estimated that banana peel has α-cellulose content of 18.7 wt. % for banana peels (Bayen, 2012), (Oliveira et al., 2017). (Yue, 2018) prepared a hybrid aerogel from banana peel and waste newspaper where the banana peel cellulose formed a sheet that reinforce cellulose fibers and enhanced its mechanical strength.

2.3 Waste Oil and Organic Solvents in Waste Water

Oil containing waste water is discharged from house hold and various industries such as leather, food, steel, paper, textile petrochemical and metal finishing industries. Direct discharge of oil containing waste water brings damage to ecological damage and also waste of oil and water resources (Mo et al., 2018). Traditional oil/water separation methods include oil skimmers, centrifugation separation, gravity separation, floatation, and absorption. Those approaches have drawbacks as they are expensive, low efficiency, tedious, processing, and even cause secondary pollution. In addition, these methods are invalid for emulsions with the droplet size below 20 mm (Zhang et al., 2017), (Yuan et al., 2018). Among those methods absorption has been considered the most effective one. It absorbs the waste and reclaim them. Several researches have been made so far on oil and organic solvent absorbing materials such as oil-absorbing fibers, 3D porous materials and oil-absorbing resin (Zhang et al., 2017).

2.3.1 Oil

Oils are nonpolar chemicals which are viscous at ambient temperature and immiscible with water but mixes with other oils. They are surface active and flammable with high content of carbon and hydrogen. Physical properties of an oil are of critical importance in determining its use. This is particularly true of the large quantity and variety of oils used in various forms as food(Riddick, Bunger, & Sakano, 1986). Oily waste water is generated from broad sources including oil industry, oil refining, oil storage, transportation and petrochemical industries all generate huge amount of oily wastewater (Yu, Han, & He, 2017).

Oils in waste water discharged into both surface and ground water resources pollute the water, changing its quality, threatening aquatic resources, human health, atmospheric pollution, and affecting crop production. There is large amount of oil discharged globally while China leads discharging the maximum allowable emission of oily waste water concentration of 10 mg/L which makes oily wastewater treatment an urgent matter in environmental engineering problems (Yu et al., 2017).

2.3.2 Organic Solvents

Organic solvents are one of the most prevalent toxic agents that pause threats to human health. They are chemicals compounds having carbon-based molecular structure that are chemically stable substances which are liquid at room temperature. Their most important property is their ability to dissolve organic matter. Organic solvents have low boiling point, high volatility, and most organic solvents are colourless (Riddick et al., 1986).

Organic solvents have wide range of applications in different areas including in extraction processes without chemically changing the material or the solvent, used in coatings, polishes, for paint thinning and removal, as cleaning agents, nail polish remover(acetone, ethyl acetate, methyl acetate), for industrial and consumer degreasers, perfumes, detergents, also in various chemical syntheses and processes (Torres, Álvarez-Hornos, San-Valero, Gabaldón, & Marzal, 2018). Organic solvents are among highly consumed industrial chemicals that can generate large quantities of solvent polluted wastewater (Dsikowitzky & Schwarzbauer, 2013). Due to their property of flammability, malodorous and potentially toxic to aquatic ecosystems it require complete elimination by wastewater treatment(Henry, Donlon, Lens, & Colleran, 1996).

2.4 Sol-Gel Process

Sol-gel method is a phase transition process in which liquid sol changes its phase to solid gel. The precursors used for sol-gel process pass through hydrolysis and condensation reactions to form the sol. The sol can be gelated into different forms of monolith, films, fibers, and monosized powders (Sajjadi, 2005). Sol-gel processing has been favourable method for its ease of control over nanoarchitecture of final product (Dervin, 2017). Sol-gel processing is advantageous mainly for its low processing temperature and molecular level homogeneity (Siqueira, Mathew, & Oksman, 2011). It is also advantageous in tailoring the nano structure of systems from initial precursors into materials with improved properties. Products of sol-gel processes have advanced properties which are prepared in forms of fine powders, films, fibers, and monoliths which may have diverse applications (Dervin, 2017).

Generally speaking there are four key stages in sol-gel processing, though additional procedures could be included to enhance characteristics of the aerogel. Figure 2 illustrates the general process flow diagram of aerogel fabrication. Each and every one of the steps in the sol-gel process contribute to the framework and structure of gel and this affects the properties which in turn affects application/purpose of the gel (Dorcheh & Abbasi, 2008).

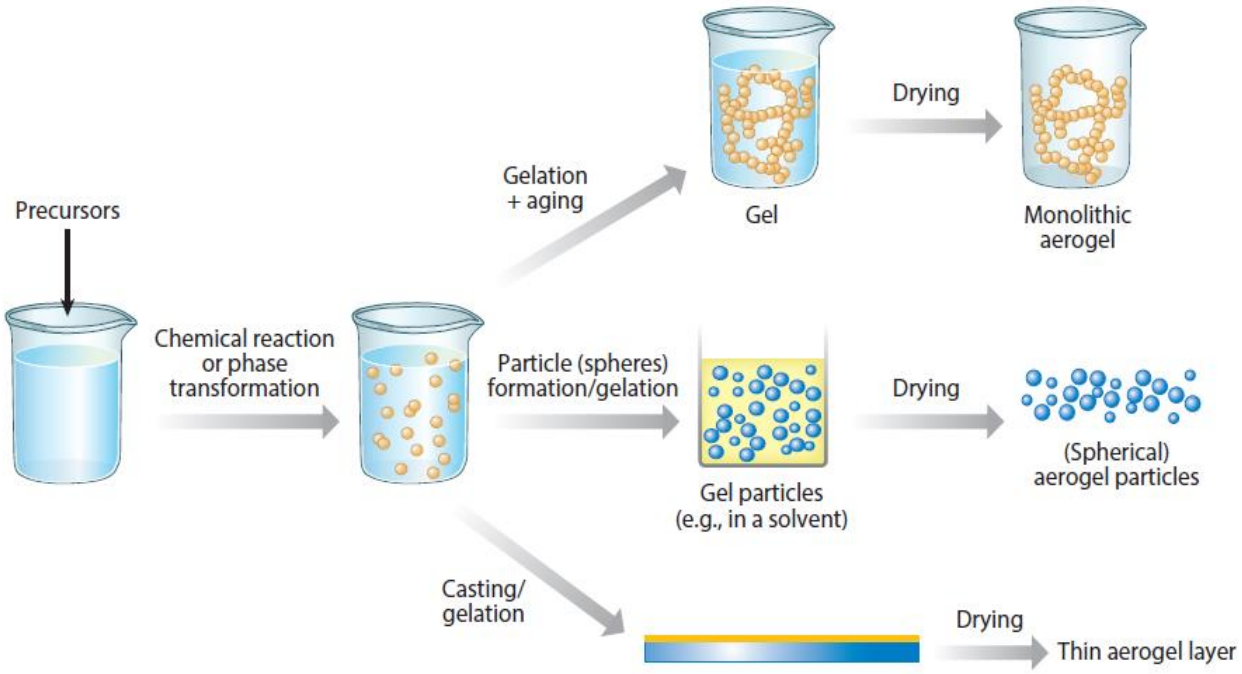

Figure 2: Main steps of aerogel synthesis (Smirnova & Gurikov, 2017)

Key stages of sol-gel:

Sol preparation: solid nanoscale particles of precursor materials are dispersed within a solvent and form a colloidal suspension.

Sol to gel transition (gelation):cross linkers are added to sol in order to initiate polymerisation and form interconnected and chained structure.

Ageing of the gel: ageing aids the increase in back bone of the gel structure and enhances the mechanical strength of gel. Ageing takes place in the mother solution.

Drying of the gel: drying is done to remove the solvent from the gel pore structures. This step can damage gel structure that it needs specific drying techniques (Dervin, 2017).

The first stage in sol-gel process is preparing colloidal suspension i.e. sol. Solid precursors in nano scale are dispersed over a solvent. Catalysts and cross linkers can be used to enhance polymerisation, hydrolysis, and polycondensation reactions. The cross linking and branching of polymeric species builds up a wet gel material of a 3D porous structure (Dervin, 2017).

Oxides, such as silica and metal oxides, organic materials such as polymers like cellulose and carbon materials, like graphene and carbon nanotubes can serve as precursors for sol-gel processes. Composites

are also interesting raw materials for sol-gel for their ability to enhance materials properties such as the gel strength (Du, Zhou, Zhang, & Shen, 2013).

2.4.1 Cellulose Dissolving Solvents

For the purpose of preparing fibers, films, and composite materials it is often preferred to directly dissolve cellulose.(Kim, Frey, Marquez, & Joo, 2005).The cellulose dissolution stage which uses a chosen treatment solvent plays a significant role in using the biomass efficiently. There are a number of solvent systems known and used for direct cellulose dissolution of which most are uncommon chemicals with strict operating conditions (Heinze & Koschella, 2005).

Most widely used and explored solvents of different categories so far, including aqueous solutions (transition-metal complexes (e.g. cuprammonium hydroxide), alkali (LiOH or NaOH), and concentrated salts ($ZnCl_2$, ammonium, or sodium thiocyanate solutions)), are among the commonly used solvents. Salt based solvents are the other groups of cellulose dissolving solvents, including molten inorganic salt hydrates (such as $LiClO_4 * 3H_2O$), which can also be used being dissolved in organic solvents (such as LiCl/N and N-dimethylacetamide (DMAc), ammonia/sodium or ammonium salt, or tetrabutylammonium fluoride (TBAF)/dimethyl sulfoxide (DMSO) are mentionable(Sen, Martin, & Argyropoulos, 2013). The recently famous and highly effective solvents are the ionic liquids (such as 1-butyl-3-methylimidazoliumchloride ([Bmim]Cl) or 1-allyl-3-methylimidazolium chloride ([Amim]Cl)) (Mäki-Arvela, Anugwom, Virtanen, Sjöholm, & Mikkola, 2010).

Cellulose dissolving solvents must be able to diffuse through the cellulose structure and affect both the crystalline and amorphous regions (Xu, Zhang, Zhao, & Wang, 2013) as can be seen on Figure 3. The crystalline regions of the cellulose structure are composed of molecules with strong intermolecular interactions of hydrogen bonding while the amorphous regions of cellulose chains entangled with each other. Therefore, the solvent system should be strong enough to with stand and disrupt the intermolecular bonding and disentangle the cellulose chains (Cao et al., 2017), (Ghasemi, Tsianou, & Alexandridis, 2017).

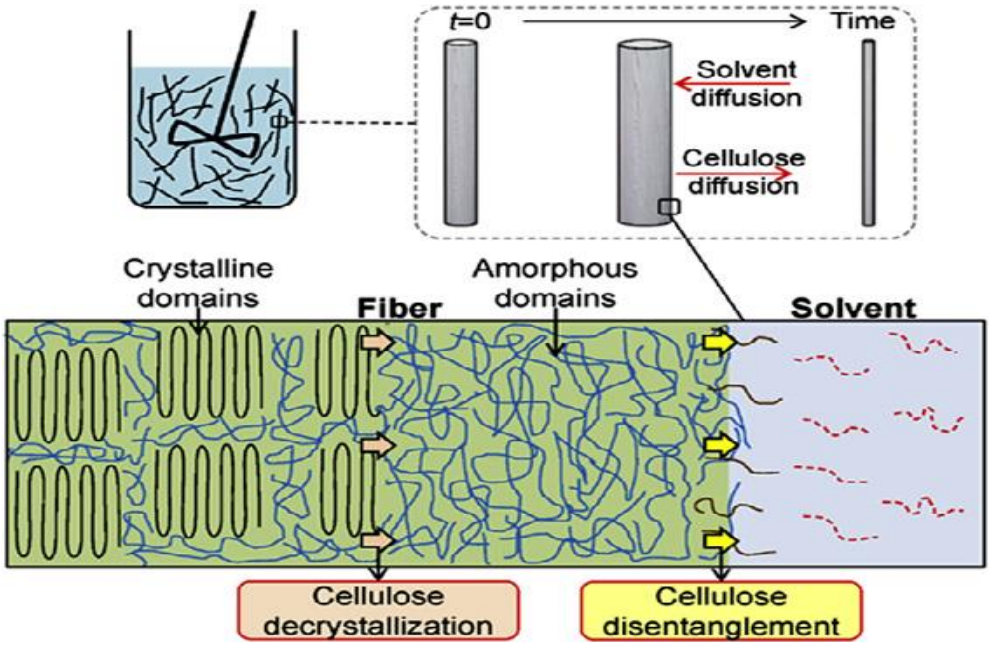

Figure 3: Dissolution processes of different regions of cellulose (Vargas-Aponte, 2017)

2.4.1.1 NaOH/Urea solvent system

Alkali solutions have been in application for cellulose dissolution purpose since 1844 when discovered by Mercer for Mercerization of cellulose and NaOH and LiOH with certain concentration range were found to effectively dissolve cellulose (Dieter Klemm et al., 2005). NaOH aqueous solution is among the cheapest cellulose solvents which can dissolve cellulose around 4 ^{o}C by destroying the intermolecular hydrogen bonds. When additives such as urea or thiourea are added to alkali solvents with proper concentration, the solubility and stability of the cellulose solution can be increased (Xiong, Zhao, Hu, Zhang, & Cheng, 2014), (Zhou & Zhang, 2000).

Studies show that urea in aqueous alkali solution can improve the solubility and stability of cellulose. Yet its specific role in the solution has not been concluded bringing controversies if urea has direct interaction with cellulose or NaOH. Xiong et al. (2014) explored the role of urea in alkali solutions and came to conclude that urea has no strong direct interaction with cellulose as NaOH solvent and has not much influence on structural dynamics of water. How Urea contributes is through van der Waals force by accumulating over the hydrophobic region of cellulose and prevent regathering of dissolved cellulose molecules. Their conclusion states that this self-assembly of cellulose and urea molecules could be facilitated by hydrophobic interactions. Therefore the NaOH/Urea solvent systems play its dissolution role as OH^- breaks the hydrogen bonds, Na^+ hydrations stabilize the hydrophilic hydroxyl groups, and urea stabilizes the hydrophobic part of cellulose (Xiong et al., 2014).

2.4.2 Solvent/coagulant exchange

Solvent exchange process, also known as solvent shifting or Ouzo effect is a bottom-up process widely used to mass produce nanoscale droplets (Binglin Zeng, Wang, Zhang, & Lohse, 2019). It is commonly applied during synthesis of organic molecules which is followed by a process that needs solute in a different solvent (Fazlollahi & Wankat, 2018). Solvent is the media in which organic crystals grow in with passive role affecting the properties of the crystals. The solvent could tune morphology and fluorescence properties. The solvent molecules are embedded within the crystal lattice having strong interactions with the neighbouring organic molecules (Wang et al., 2020).

Initial material composition changes as it is immersed in coagulation bath and solvent diffuses in the bath as it is gradually replaced by nonsolvent. The fast solvent-coagulant exchange occurs with large repulsive force between polymer gel and coagulant, causing precipitation at the interface. The choice of the appropriate coagulation medium represents a significant aspect in porous material preparation. This solvent should not dissolve the crystal but should be miscible with the liquid phase of the system (Zare & Kargari, 2018). All aerogel production processes need at least one solvent exchange step. Mass diffuses through gel which limits the process speed and particle size (Schwertfeger, Frank, & Schmidt, 1998).

In this method, homogeneous polymer solution is immersed in a suitable coagulant where suspended polymer fibers could be drawn to the back bone of the polymer and facilitate gelation process. Common antisolvents include water, ethanol, or isopropanol which can coagulate the polymer over a period of time (Onwukamike et al., 2019). Enhanced aggregation of polymer can be a result of ethanol induced decrease of inter-polymer repulsion (O'Connell et al., 2006).

2.4.3 Aging

Ageing is consecutive step after solvent/coagulant exchange where gelation process proceeds. Gelation is when solution loses its fluidity and gains elastic solid property. During aging chains of bonds form the polymer spanning cluster that restrains pore liquid. This process involves no exotherm, endotherm or any chemical evolution in the gel system. During the period of aging the process taking place can be polymerization, coarsening, or phase transformation. Polymerization is a condensation reaction that increases the connectivity of network. The reaction stiffen and strengthens the network by creating new bridging bonds (Brinker & Scherer, 1990). The coarsening is also known as Ostwald ripening in which molecules dissolve from energetically less favoured site on the network and accumulate on a place that is energetically more favoured. Therefore the network strengthens and coarsens (Maleki, 2016).

In general the aim of aging is to mechanically reinforce the weak solid skeleton generated by sol-gel process. Water or alkoxysilanes can be used for aging that facilitate surface reaction especially involving residual hydroxy/alkoxy groups. These reactions are supplemented with condensation reactions and dissolution/reprecipitation of the solid skeleton (Aegerter, Leventis, & Koebel, 2011). That is the gel network grows further in the gelation solvent which contains reactive species (like -OH) or unreactive monomers that condense onto the gel network. Aging can take hours to days by soaking in a preferred solvent that may be in the initial sol or a different solvent under a controlled aging conditions. Time, temperature and pH affect the general aging process. Textural properties of the gel such as porosity, pore size, and surface area change as it ages (Maleki, 2016).

2.5 Drying Techniques

The gel formed from sol-gel process is finally dried to produce aerogels. Generation of a 3-D porous network of the gel material is a critical aspect in the aerogel production process. The same gel should then be dried without losing the original porous structure (Maleki, 2016). This makes drying of the gel from sol-gel, the most significant process involved in preparing aerogels. Different methods of drying gels have been effectively implemented so far to prepare aerogels. The common three main routes of gel drying are: freeze-drying (necessitates to bypass the triple point), Ambient pressure drying (implies crossing the liquid–gas equilibrium curve), and supercritical drying (necessitates to bypass the critical point) (Aegerter et al., 2011).

2.5.1 Supercritical Drying

This is the most efficient approach to dry wet gels under supercritical conditions. The wet gel is first placed inside pressure vessels and the pressure and temperature of the vessel reach over the critical points of the pore solvent. At these points the solvent converts to a gaseous phase and evaporates (Maleki, Durães, & Portugal, 2014).The advantage of supercritical drying is mainly due to the absence of capillary stresses. Therefore the dried gels will be crack free solid gels. Critical drying depends on the solvent used to impregnate the wet gel. The most common one is liquid CO_2 (Maleki, 2016).

Supercritical drying can be done at ambient or elevated temperatures commonly referred as low temperature supercritical drying (LTSCD) and high temperature supercritical drying (HTSCD), respectively. LTSCD is also known as CO_2 exchange, described by phase diagram of CO_2 on Figure 4 (b) below, that replaces the pore solvent (Tewari, Hunt, & Lofftus, 1985). This exchange of pore solvent results in the formation of hydroxyl groups on the surface of aerogels. On the other hand the HTSCD completes drying first by reaching the critical temperature and pressure of the pore solvent and evaporate.

During the drying process, the solvent reacts with hydroxyl groups on gel surface and forms methoxyl groups. This makes the aerogels hydrophobic (Dorcheh & Abbasi, 2008).

2.5.2 Ambient Pressure Drying

Ambient pressure drying also called subcritical drying, is an inexpensive, simple, and safe technique for gel drying purpose under ambient pressure. It is suitable for mass production. The drying relies on surface modification at ambient pressure by exchanging the pore solvent with another solvent with low surface tension so that to circumvent the capillary stresses endured by the pore walls. The other solvent diffuses into the gel, replace polar surface groups with nonpolar groups, and chemically modifies the surface of the gel (Smitha et al., 2006). This surface modification disrupts further condensations after being compressed by capillary stresses. At the end of drying the nonpolar neighbouring groups that are repulsive, can recover the original dimension by spring-back effect (Maleki, 2016).

2.5.3 Freeze Drying

Freeze drying is simple, economical, and environmentally safe drying technique used to prepare aerogels with reasonable porous structures. Figure 4 (a) clearly shows the phase transformation that takes place during freeze drying. The drying starts by freezing the pore liquid inside the gel followed by sublimation process under low pressure. The freezing rate and the crystal shape and size affect the end product properties such as pore size and quality. Rapid freezing forms small ice crystals resulting in small pore size and high pore surface area. On the contrary a slow freezing results in larger ice crystals that forms large pore sizes(Fricke & Emmerling, 1992).

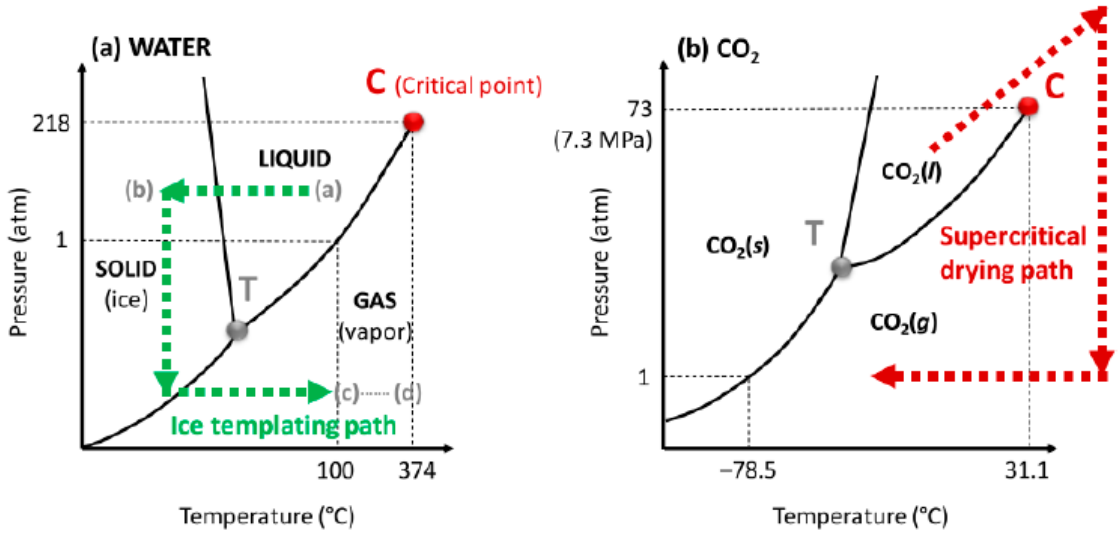

Figure 4: Phase diagrams of freeze-drying (**a**) and supercritical-drying (**b**) superposed on water and CO_2 (Illera, 2018)

Freeze drying removes all moisture entrapped in gel and leaves a web of solid fibers (Gurav, Jung, Park, Kang, & Nadargi, 2010). The drying process depends on the capillary pressure(Pc) inside the pore which relates to surface tension, pore volume, and surface area (Brinker & Scherer, 1990). The final aerogel properties including morphology, are dependent on freezing conditions, solid particle size and concentration in the suspension, and the self-organizing behaviour of the precursor fibers during freeze drying (Zanini et al., 2018).

Aerogels prepared by freeze drying sometimes partially fail to maintain their porous structure due to the ice formation inside the pores. This results in high volume macroporousity, larger extent of shrinkage, and lower specific surface area than aerogels of supercritical drying. For aerogels with good properties, the pre-drying treatments like aging and solvent exchange can be manipulated for better gel structure (Maleki, 2016).

2.6 Applications of Aerogels

Aerogels have tremendous potential in a wide range of applications in which its high porosity and high surface area play major roles. Industrial aerogels production so far is mainly limited to silica-based, carbon, and some organic based aerogels. Currently, the main market application of aerogels is thermal insulation, because aerogels are the best thermal insulating material in the market besides vacuum insulation panels. Most common applications of aerogels include thermal insulation, waste water absorption, medical implants, cosmetics, and catalysts. Aerogels can also serve as carrier materials for catalysis**,** electrocatalysis**,** and biocatalysts, etc(Smirnova & Gurikov, 2017).Aerogels also have applications in home buildings, vehicles, pipelines, packaging electronic components, and in capacitors where they serve as humidity sensors, and IR detector. It also has applications in the Cosmetics, pharmaceuticals (drug delivery), apparel & sports ware (Tennis rackets, Security shoes, Sports shoes), and for space materials such as space suits (Ratke, 2006).

Aerogels have applications in environmental clean-up applications both for air and water cleaning. The porous aerogel material has applications in a selective CO_2 capturing technology to minimize the emission of CO_2 as a main and primary greenhouse gas into the atmosphere. Aerogels are also capturing of hazardous volatile organic vapour exhausts from industries and motor vehicles such as benzene, toluene, ethylbenzene xylene which are also known as ‘‘BTEX”. The aerogel properties of micro/ meso/macroporous it with high surface area, and tailorable pore surface chemistry are reported to be promising alternative absorbents with high uptake capacities for the removal of the toxic pollutants meet adsorption requirements (Maleki, 2016).

2.6.1 Aerogels as Sorbent Materials

In recent years, the application of aerogel sorbents in sample preparation techniques has increased remarkably. These materials have unique features as sorbents and have shown good results in various sample preparation techniques. These unique features include a high surface area, low density, high porosity, and thermal stability, which make aerogels suitable as sorbents in analytical applications. In addition, it is well known that the efficiency of microextraction techniques mainly depends on the extraction material. Aerogel sorbents have been considered as suitable options to improve extraction and sample preparation techniques for different compounds present in complex matrices (Jalili, Barkhordari, & Heidari, 2019).

There are four types of standard sorbents. films, sheets, pads, etc are categorized as type I sorbents. Their length and width is much larger than their thickness. Type II are unconsolidated particulate materials like powders or loose particles. Type III are enclosed sorbents including pillows and booms. The sorbent material is confined by an outer permeable material. The other type is type IV sorbents that have an open structure that is suitable for highly viscous oils to intrude through it. such as pompoms with an open structure that allows the intrusion of high viscosity oils (Alireza Bazargan, 2014; Pintor, Vilar, Botelho, & Boaventura, 2016).

2.7 Hydrophobic Modification

CBA materials, being products of cellulose fibers, are hydrophilic materials. This property lowers CBA selectivity performance as an absorbent and by that decreases its durability and shelf life. Therefore hydrophobic surface modification of CBA can alleviate the matter and enhance CBA performance.

Hydrophobic materials are materials having contact angle with water and aqueous solutions more than 90^{o}. The major feature is instability of thin wetting water layers on surfaces without a special affinity for water. Hydrophobicity is caused by near-surface layer properties and structure of a few nanometres thick. The unique set of functional properties include corrosion-resistant, waterproof, and stable against biofouling and inorganic/organic pollutants. Fluid flows on hydrophobic surfaces with ease (Boinovich & Emelyanenko, 2008).

Various hydrophobising chemical treatments can change chemical composition of material surfaces and achieve contact angles less than 120°. Chemical structure and surface roughness influence the effectiveness of hydrophobic modification by creating low surface energy and micro-nano structure (Boinovich & Emelyanenko, 2008). Figure 5 illustrates hydrophobicity level of surfaces, based on their surface-water contact angle.

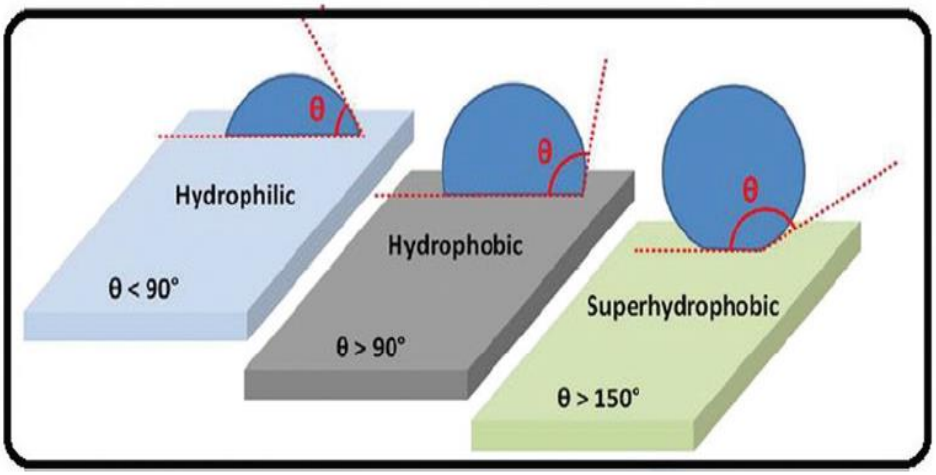

Figure 5: Schematic illustration of hydrophilicity-hydrophobicity properties of surfaces (Liu et al., 2016)

Modern hydrophobic treatment has no adverse effect on the properties of bulk material which is advantageous to achieve desired product quality (RAŽIĆ, Čunko, Bukošek, & Rolich, 2010).Among the methods of hydrophobic modification are, chemical etching, solution-immersion process, spray coating, laser electrodeposition, and template deposition where the latter two require no surface roughening. The important properties of hydrophobic modification processes are simplicity, time consumption, cost, versatility, durability, and storability (Ali, Qasim, Malik, & Murtaza, 2018).

2.7.1 Candle Soot/Acetone

Dating back to 1907, Olivier observed superhydrophobic phenomena on surfaces consisting of soot, lycopodium powder, and arsenic trioxide. Thereafter, the first synthetic super-water- repellent surfaces to mimic the lotus leaves were fabricated in 1996 by introducing high roughness onto alkyl ketene dimer films (Lin, Park, Choi, Heo, & Hong, 2019). These materials have also been successfully applied in superhydrophobic and superamphiphobic coatings, as high absorbance materials for solar collectors, and as adsorbents for various organic molecules, pollutants and dyes (Puneet Azad, 2019). Candle soot (CS) are composed of carbon nanoparticles widely used, particularly as a robust superhydrophobic coatings (Deng, Mammen, Butt, & Vollmer, 2012). Candle soot can be dispersed on alcohols, such as ethanol,

acetone and isopropanol to form a homogeneous solution and enhance durability (Zhao, Zhao, Yan, & Liu, 2018).

Candle soot are low-cost and high-efficiency photothermal surfaces that naturally possesses structurally desirable features that provide hierarchical nano/microstructures to surfaces. The incomplete combustion naturally forms nearly perfect hierarchical structure from nanoscale carbon material assembles. Such a hierarchical structure makes the soot deposited on substrates an ideal superamphiphobic coating (Deng et al., 2012).

2.8 Literature summary

Table 2: Summary of similar literatures

Reference	**Raw material**	**Process**	**Results**
(Nguyen et al., 2013)	Recycled paper cellulose fibers	• Sol-gel process with sodium hydroxide/urea solvent • Methyl trimethoxy silane (MTMS) • Freeze dried	• Sorption capacity for different crude oils, 18.4, 18.5, and 20.5 g/g
(Thai et al., 2020)	Sugarcane bagasse	• Bleaching with sodium hydroxide and hydrogen peroxide, • PVA cross linking with curing at 80 ^{o}C • MTMS coating improves • Freeze dried	• Sorption capacity up to 25 times the initial weight
(Onwukamike et al., 2019)	Recycled microcrystalline cellulose and cellulose pulp	• Sol-gel dissolution with DBU, TMG, and DBN • Solvent switched to CO_2 • Freeze dried	• BET specific surface areas ranged between 19 and 26 m_2/g

DBU = 1,8- Diazabicyclo, TMG = Trimethylglycine

Chapter III

3. Materials and Methods

3.1 Materials

The raw materials collected for this research were waste paper, banana fruit peels, and unbleached and undyed waste cotton fabric (100 % cotton) separated from solid waste stream. Analytical grade sodium hydroxide (99.8 %), extra pure Urea 99.9 %, analytical grade ethanol (99 %), extra pure acetone (99 %), and distilled water were purchased from local chemical stores. Candle soot was also used which was collected from burning paraffin candle.

3.2 Methods

Cellulose-based aerogel was produced following two steps. The first step was conventional sol-gel process to prepare gel from the mixed solid waste. The second step was to freeze dry the gel and fabricate cellulose-based aerogel.

The raw materials, i.e. banana peel, waste paper, and waste cotton fabric, were washed, air dried and size reduction was done which will promote formation of a homogeneous sol. The banana peel was size reduced to less than 125 µm while waste paper and waste textile cotton fabric were mechanically size reduced to soft cottony nature in the micron scale. NaOH/Urea/Water solvent was pre-cooled to -12 ^{o}C. The sol-gel precursors (WP:WCF:BP) in a proportion of 1:1:0.1 (Onwukamike et al., 2019), were dispersed on 100 ml NaOH/Urea/water (7:12:81) solution under continuous stirring (Jie Cai,2005).

The cellulose extraction from precursors was investigated at different precursor to dissolution ratio of (1.1 g:100 ml), (2.2 g:100 ml), and (3.3 g:100 ml) and different dissolution time (1, 2, and 4 hours) (Thai et al., 2020), (Vadahanambi S., 2020). Based on these factors total of 9 runs were conducted. Dissolution took place in acetone/ice bath to maintain the dissolution temperature at less than 10 ^{o}C. Table 2 below lists combinations of the two factors and the total performed experimental runs. Then the homogeneous solution formed from dissolution was placed in a refrigerator for two days to allow gelation. Afterwards, the frozen homogeneous solution was thawed at room temperature for hours followed by immersion into ethanol for 4 hours for coagulation. Solvent exchange was carried out by immersing the sample in deionized water (DI) for more than 2 days in a mold. Finally freeze-drying was carried out to prepare monolithic cellulose-based aerogel using benchtop freeze dryer LyoQuest -55/230 V, 50Hz. Gels were freezed to -18 ^{o}C for 12 hours prior to freeze drying. The freeze drying was performed at -50 ^{o}C and 0.001 mbar for 3 days. Then dried samples were placed in a desiccator for 3 days to avoid any chances of capturing moisture. Figure 6 schematically shows the entire sol-gel-drying process discussed above.

Table 3: List of experimental parameters and levels

Level	Time(hr.)	Precursor/solvent ratio (g/ml)
R_1t_1	1	1.1:100
R_2t_1	1	2.2:100
R_3t_1	1	3.3:100
R_1t_2	2	1.1:100
R_2t_2	2	2.2:100
R_3t_2	2	3.3:100
R_3t_3	4	1.1:100
R_2t_3	4	2.2:100
R_3t_3	4	3.3:100

Time = (t_1= 1hr, t_2= 2hr, t_3= 4hr), precursor/solvent Ratio = (R_1=1.1g:100ml, R_2=2.2g:100ml, R_3=3.3g:100ml)

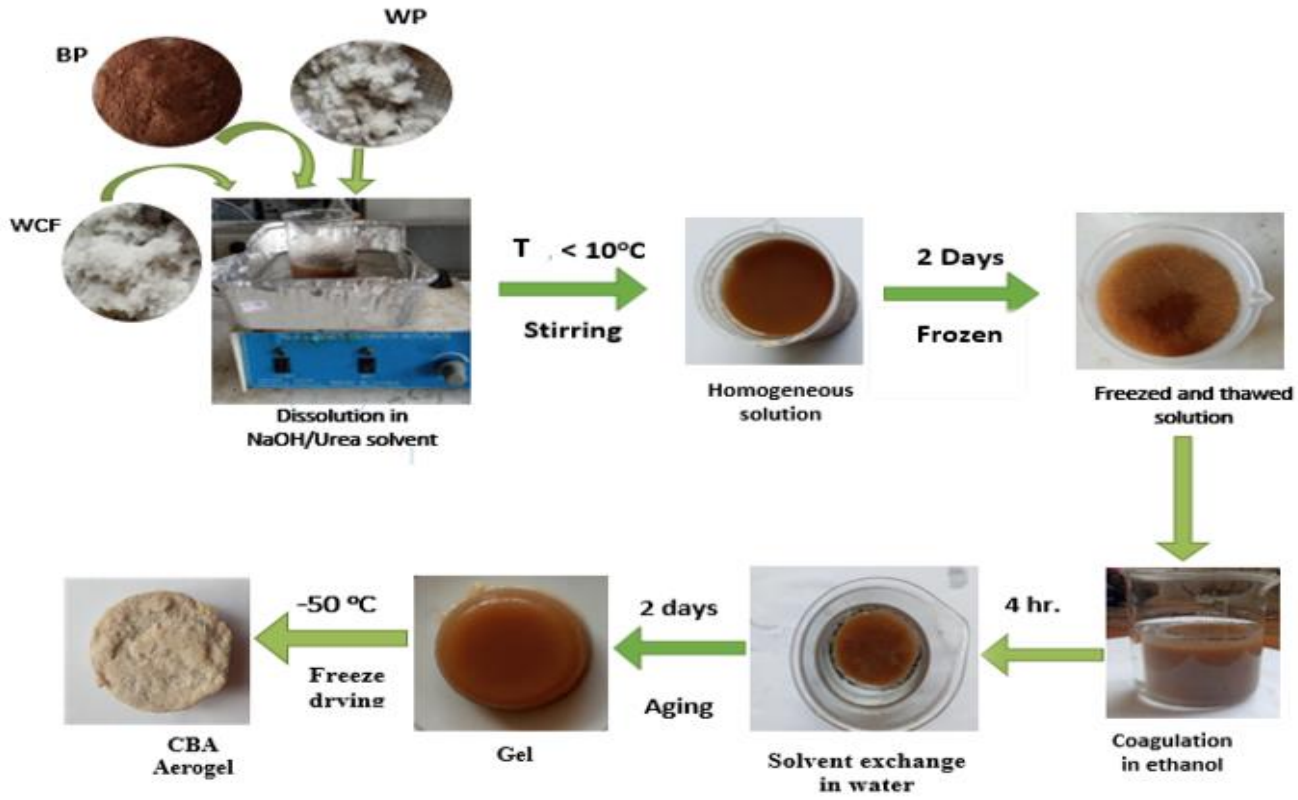

Figure 6: Schematic presentation of Cellulose-based aerogel fabrication from mixed organic solid wastes

3.3 Hydrophobic Coating of Cellulose-based Aerogel

Hydrophobic modifications were made according to the work of (Puneet Azad, 2019). Candle soot was prepared by burning a paraffin candle over the surface of silicate beaker and scratched off it. 30 mg of the soot was mixed with 100 ml acetone followed by 30 min of sonication. The CBA was dipped in the prepared CS–acetone solution and left for 10 min. It was then dried under a 50 WIR lamp at 75 ° C then further dried in oven at 75 °C. Figure 7 schematically presents this process.

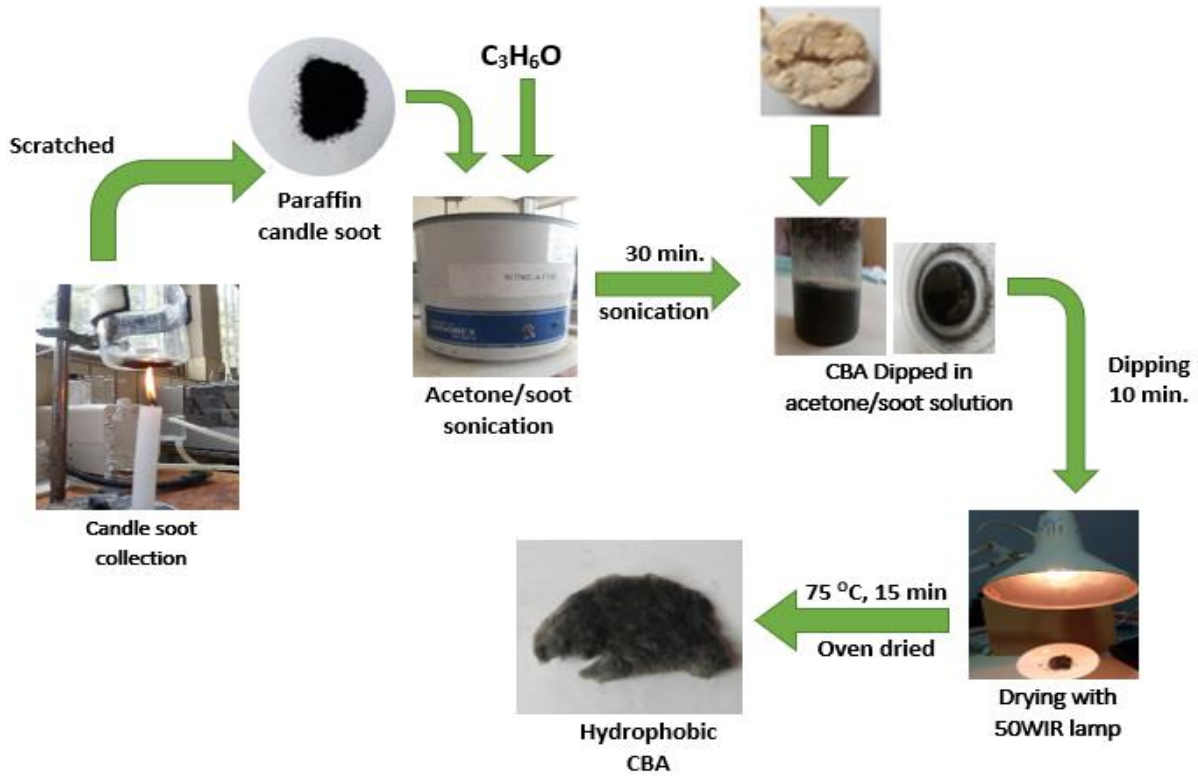

Figure 7: Flow diagram of hydrophobic modification for CBA

3.4 Characterization of Cellulose-based aerogel

The final fabricated cellulose-based aerogels was characterized for its important properties as a sorbent such as its, density, porosity, morphology and specific surface area which influences the efficiency of CBA material as an absorbent material.

3.4.1 Apparent Density (Bulk density) of CBA

Density is a characteristic property of aerogels which was estimated gravimetrically by an adaptation of ASTM D3575-14 standards (Zanini, 2018). Measured mass of CBA was placed in a measuring cylinder containing distilled water. The water volume in the beaker increased slightly as the CBA was immersed. The displaced water volume and mass of CBA were measured used to calculate density.

$$\boldsymbol{\rho = m/v}, \qquad \text{(eq.1)}$$

Similar tests were performed multiple times and the average value was calculated.

3.4.2 Porosity Measurement

The porosity (% Φ) of the aerogel is measured using the formula:

$$\boldsymbol{\%\ \Phi = \left(1 - \frac{\rho\ a}{\rho\ b}\right) x\ 100} \qquad \text{(eq. 2)}$$

where ρ_a is the aerogel density and ρ_b is the micro crystalline cellulose density (1.5 g/cm^3) (Jin et al., 2015).

3.4.3 Nitrogen Sorption Measurement

A 0.05 gram of sample was weighed using analytical electronic balance (AD-300-3, 0.001 resolution) for all run and placed in to a sample holder. These samples were put in to the preparation unit of the surface area analyser (Horiba 9600 series) where all samples were subjected to 200 °C temperature for 45 minutes to remove (degas) the moisture content. After cooled off, each sample were weighed again and the weight was recorded. These prepared samples were transfer to the surface area test part of the BET. The environment of the system was filled with helium gas by replacing the air available in the sample holder. The system was calibrated each time it runs by injected 1 cc (cubic centimetre) nitrogen gas. Thereafter, a mixture of 20, 30 and 50% of nitrogen and helium of 2 bar each were injected to the sample intermittently. Simultaneously, the sample was cooled indirectly by liquid nitrogen (-196 °C) during which nitrogen gas behaved like liquid and was adsorbed and formed monolayer on each surface of the sample. When the cooling system was removed the adsorbed nitrogen gases desorbed and were accounted

by conductivity meter detector. Based on the single nitrogen molecule surface area and the number of the nitrogen adsorbed-desorbed of the multipoint data, the surface area of each sample was determined.

3.4.4 Morphological Analysis

Field emission scanning electron microscope (FE-SEM) was used to investigate the morphology of the fabricated aerogel. Inspect F-50 FE-SEM American model for general purpose machine was used. The images were magnified at 1078 x operated at an accelerating voltage of 10.00 kV.

3.4.5 Fourier Transform Infrared Spectroscopy (FTIR) Analysis

This characterization was intended to examine the effectiveness of hydrophobic modification done. Although FTIR spectra cannot give quantitative information/measurements of the degree of hydrophobicity. But it can reveal the qualitative information on surface modification and identify the attached functional groups on the fabricated CBA, specifically the attached O-H group. FTIR analysis was done using spectrum 65 FTIR (Perkin Elmer) in the wave number range 4000-400 cm^{-1} using KBr pellets.

3.4.6 Thermal Stability Measurement

Thermogravimetric tests were done to find the thermal stability of CBA materials. Tests were conducted from room temperature to 700 ^{o}C temperature range increasing at a heating rate of 10 ^{o}C/minute. TGA shows the weight loss of sample as the temperature increases while the DTA shows any change detected in specific heat or enthalpy.

3.5 Absorption Efficiency Test and Regeneration

The fabricated CBA was tested for both its sorption capacity and removal efficiency on oils and organic solvents. Oils i.e. cooking and Quartz 5000 20W-50 engine oil, and organic solvents i.e. benzene and ethanol, were used for the test.

3.5.1 Sorption Capacity Test

ASTM F726-17 sorbet performance test method (Zanini et al., 2018) was used to investigate the sorption capacity of CBA with the most suitable properties for pollutant removal application via absorption process. Accordingly, at room temperature, a CBA with a given mass was immersed into 20 ml organic solvents (ethanol and benzene) and oil (cooking oil and motor oil). The static sorption process was maintained for 15 minutes contact time between sorbent and oil/organic solvent. After that, the saturated sorbent was physically separated from the liquid, followed by a dripping time of 30 s and weighed quickly.

The sorption capacity of the CBA was evaluated using the following formula: where CA is sorption capacity ($g.g^{-1}$), m_i is initial mass (g), and m_f is final mass (g).

$$CA = \frac{mf - mi}{mi} \qquad \text{(eq. 3)}$$

3.5.2 Removal Efficiency Test

The removal efficiency of CBA was tested in a heterogeneous medium of water/oil and water/ organic solvent solutions. The quantity of oil/organic solvent previously estimated from sorption tests oil/organic solvent was added to a 100 ml of distilled water. Adaptation of ASTM F 726-17 (Zanini et al., 2018) was used for removal test in which CBA aerogels were placed in the heterogeneous medium for 15 minutes. The sorbent was removed from the media leaving it to drain for 30 seconds of drippling time. The concentration of pollutant in waste water after every cycle was measured using single beam spectroscopy (JASCO V-770 UV-vis-NIR) performed at room temperature. The calibration curve method was used which is alternative approach that avoids liabilities of Beer-Lambert's law.

At first, a standard curve was made by preparing samples of known concentration including the initial concentration used for removal efficiency test and running UV/VIS test to get their absorbance values. Hence the calibration curve was determined and the calibration equation was extracted thereby, where the correlation value (R^2) was within the acceptable range ($0.95 < R^2 < 0.98$). From the equation, remaining pollutant concentration was calculated which was then used to find removal efficiency.

After each cycle, the aerogel was regenerated and reused for the next cycle. For the regeneration combined squeezing and heating of the aerogel were done. The CBA containing oil/organic solvent was first squeezed to remove most of the contaminant then it was dried at 80 ºC to remove the remaining contaminant. The combination of the steps helps in maintaining the porous structure of the aerogel. This method was adapted from (Zhu et al., 2017).

Chapter IV

4. Results and Discussion

The synthesized cellulose-based aerogel was a spongy, light weighted, and flexible material which are the basic aerogel physical properties. The important properties of CBA were characterized and the effect of parameters were examined. Finally the performance for a number of oils and organic solvents removal from waste water were determined.

4.1 Apparent Density (Bulk density) of the CBA

After gravimetrical estimation of the aerogel bulk density, the density value of all samples/runs were all determined to be less than 0.5 g/cm^3 which lies within the range of aerogel density. The lightest aerogel with lowest density of 0.127 g/cm^3 was synthesized at 4 hours of dissolution time with 2.2 g:100 ml precursor/solvent ratio . This value indicates how light the material is and that most of the space in the material is filled with air. Compared to other researches that used alkaline/urea solvent systems, it is relatively higher (Thai et al., 2020), (Zanini et al., 2018). This could be attributed to nature of porosity that determines the amount of empty space inside the CBA. Yet the CBA was light enough to float over water. The CBA became less denser as more time was given for cellulose dissolution which chemically fibrillates the cellulose precursors for longer period of time. The mean apparent density was 0.259 g/cm^3 and the standard deviation was 0.092 g/cm^3 which measures the variability and how far values lie from the mean value.

4.2 Porosity Analysis

Porosity is the fundamental characteristic property of aerogels that determines other important characteristics and their applications. The density of aerogels fabricated at different conditions were evaluated from the density of aerogel and the precursor, i.e. cellulose. Substituting these values into (eq.2), the highest porosity achieved was 91.5 % by the CBA fabricated at 4 hours dissolution time and 2.2 g:100 ml precursor/solvent ratio. Table 4 lists the porosity values of all runs. This shows that the drying process had sufficiently preserved the initial volume of the gel leaving most of the aerogel volume to be empty/air. The mean porosity of the samples was 82.7 %. The standard deviation of porosity of each run is 37.38%.

The dissolution time has affected the porosity incrementally, which indicates that longer contact time between precursor and solvent results in better fibrillation and dissolution of cellulose fibers. The effect of ratio, on the other hand, was inversely proportional for the majority of the results except for R_1t_3 and R_2t_3. The concentration loaded could have increased the mass, thereby the density (Thai et al., 2020).

Density is determinant for porosity of aerogel, that the denser the CBA the less porous it becomes. The porosity level of the two samples that reject the inverse relationship of porosity and ratio, have porosity in close range, 88 % and 91.5 %, respectively. The porosity-ratio pattern seen at the mentioned points could be due to the lower ratio of R_1t_3 where precursors overwhelmed and suspended in the NaOH/Urea solvent. This contributes less to the network formation of the CBA, though the higher dissolution time was advantageous in fibrillating cellulose and creating highly porous CBA.

4.3 Specific surface area analysis

BET surface area was measured over the relative pressure range of $0.179 < P^o/P < 0.449$. The highest BET surface area of CBA was recorded to be 192.24 m^2/g for the CBA synthesized at conditions of 4 hours of dissolution and 2.2 g:100 ml precursor/solvent ratio. The mean specific surface area is 147.93 m^2/g and the standard deviation of the specific surface area values is 33.79 m^2/g. Surface area is highly influenced by porosity level which affected by dissolution time and precursor/solvent ratio. The loss of smaller pores during freeze drying and aging could have affected the surface area of CBA. The result is in a reasonable agreement with the range of previously reported values. Table 3 compares the specific surface area of freeze-dried CBA prepared by similar researches.

Table 4: Specific surface area of freeze dried cellulose based aerogels reported in literature

Preparation Method	**Reference**	**Specific surface area (m^2/g)**
Sol-gel process using denim waste precursors and freeze dried	(Zeng, Wang, & Byrne, 2019)	133
Recycled cellulose was used for sol-gel process and freeze dried	(Jin, Nishiyama, Wada, & Kuga, 2004)	70–120
Nano fibrillated cellulose from wood fibers used in sol-gel process and freeze dried	(Sehaqui, Zhou, & Berglund, 2011)	153–284
Aerogels prepared from commercially available eucalyptus pulp and N-methyl-morpholine-N-oxide solvent	(Innerlohinger, Weber, & Kraft, 2006)	50-420
WC, WP, and BP were used in sol-gel and freeze dried	This study	192.24

The density, porosity, and specific surface area of all CBAs synthesized by varying the chosen parameters are summarized on Table 4.

Table 5: Summary of properties of CBA fabricated at different processing conditions

Exp. Run	Density (g/cm^3)	Porosity (%)	Specific surface area(m^2/g)
R_1t_1	0.282	81.2	145.8
R_2t_1	0.307	79.5	117
R_3t_1	0.418	72.1	98.65
R_1t_2	0.244	83.7	149
R_2t_2	0.183	87.8	174.42
R_3t_2	0.354	76.4	108.12
R_3t_3	0.18	88	183.79
R_2t_3	0.127	91.5	192.24
R_3t_3	0.24	84.1	162.4

The samples with the highest porosity level and specific surface area, i.e. R_2t_3, was chosen for hydrophobic modification and for chosen oil and organic solvents removal efficiency test. SEM, FTIR and TG/DTA characterizations for this sample are discussed below.

4.4 FE-SEM

The FE-SEM images revealed the fibrillation of cellulose fibers from precursors and the network formed by the fibers. The images shown in Figure 9 are SEM images of CBA synthesized at 4 hours dissolution and 2.2 g:100 ml precursor/solvent ratio. It's observed in this SEM image, that compact cellulose fibers in micrometric scale intertwined with each other creating an opening with interstices shape. The interstices pore shapes might have been enhanced by the short fibers from WC precursor and the mechanical fibrillation of precursors that could have shortened the cellulose fiber length.

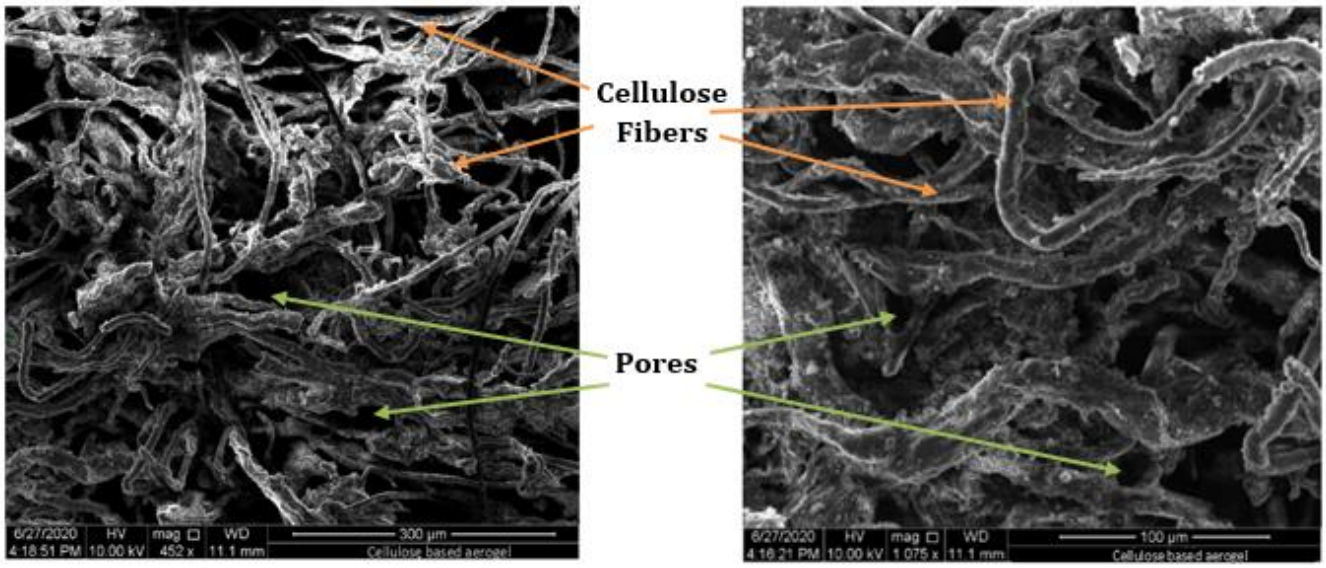

Figure 8: FE- SEM images of cellulose-based aerogel (R_2t_3) at resolution of 300 µm (left) and 100 µm (right)

The pore walls, i.e. the fibers, are in the micrometric level that are not considered thine compared to reports from other researches. The pores created as the fibers intertwined with each other i.e. the dark areas in the SEM images above, are relatively large. Finer pores probably have been destroyed during freeze drying process as the water ice were forming which later sublimated to be gas. This phase transition process causes rise in capillary stress inside the pore which eventually creates pore cracking (Maleki, 2016).

The pores exhibit less uniformity and tortuously interconnected microporous network of cellulose fibers were formed. The uniformity of pores might be affected during the cellulose dissolution and gelation steps. This and the thermodynamic properties of NaOH/Urea/water solvent system that might have induced the gelation of the solution with time and temperature increase could have affected the porosity of the CBA. The banana peel micro sheets seen on SEM images of the study by (Yue, 2018) were not observed on the SEM images of this work. This could be related to the proportion of the precursors that

the presence of WC has dispersed the BP micro sheets. This could have reduced the reinforcing effect of BP micro sheets which later affects the waste removal efficiency of CBA after regeneration.

The characterizations from here on are done on the single sample that has results of the lowest bulk density, highest porosity, and specific surface area.

4.5 FTIR Analysis

FTIR test was done on CBA with optimum properties (i.e. high porosity and specific surface area) before and after hydrophobic modification (Figure 10). Both samples before and after hydrophobic modification show almost similar patterns on the FTIR spectra. The CBA FTIR spectra shows a peak around the 3424 cm^{-1} which indicates the presence of the O-H stretch. This peak significantly decreased after modification which indicates that O-H groups on the surface have been replaced. C-H stretch is seen at 2915 cm^{-1} and 1618 cm^{-1} later shifted to 2921cm^{-1} and the band1622 cm^{-1} respectively. The vibration at 2368 cm^{-1} might be due to the presence of O-H stretching due to absorbed water. This band later disappeared on the modified CBA spectra. Appearance of the peak around 1082 cm^{-1} later shifted to 1024 is attributed to C-O stretching. The small vibrations around 1436, 1024, and 874 cm^{-1} indicate the presence of C-O and C-C bending vibrations (Khan et al., 2018) (P. B. Wagh, et al,. 2015).

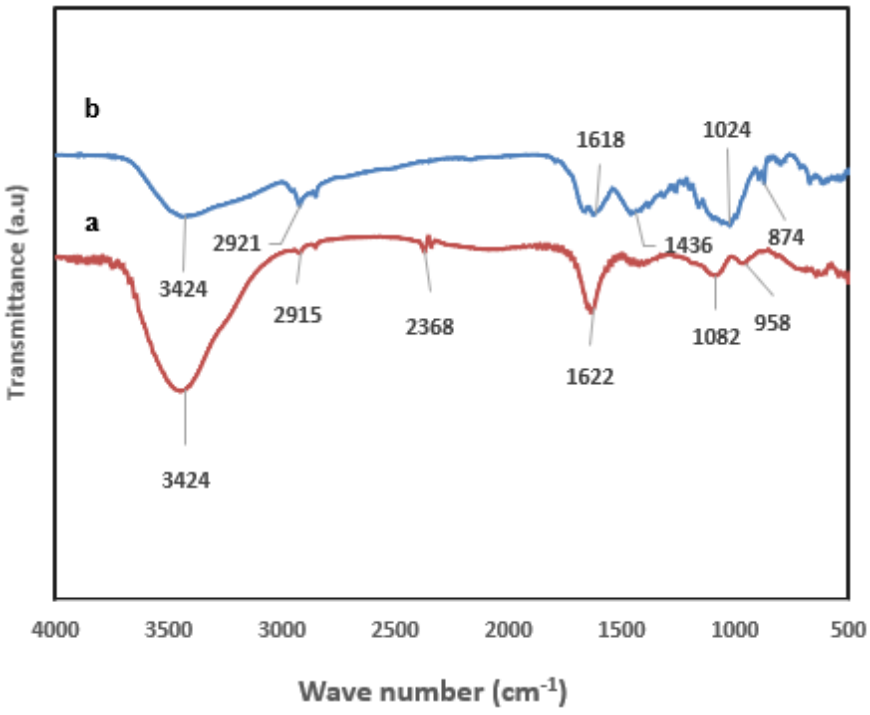

Figure 9: FTIR spectra of CBA before (a) and after hydrophobic modification (b)

The FTIR spectra of CBA after hydrophobic modification shows that the peak a t3424 cm^{-1} has been significantly weakened and less-stretched, which is responsible for the presence of -OH groups. The intensity decrease could be caused by the carbon nanoparticles of the carbon soot/acetone solution successfully attached to -OH groups of the CBA. The increased vibrations at 1436 to 874 cm^{-1}can be caused by C-C bonds of carbon nanoparticles that have been assembled by the hydrophobic modifications. This can be evident that the hydrophobic property of CBA has been highly improved. The improvement gives the aerogel more durability and selectivity properties which in turn makes it more efficient for oil and organic solvent removal from waste water.

4.6 Thermal Stability Analysis

Thermogravimetric tests were done to find the thermal stability of CBA materials with the optimum properties. Tests were conducted for the sample with the best characteristics i.e. highest porosity and specific surface area, from room temperature to 700 ^{o}C temperature range increasing at a heating rate of 10 ^{o}C/minute. TG/DTA curve (Figure 11), presents the thermal effect on sample weight, i.e. the TGA curve shows the weight loss of sample as the temperature increases while the DTA curve shows any change detected in specific heat or enthalpy.

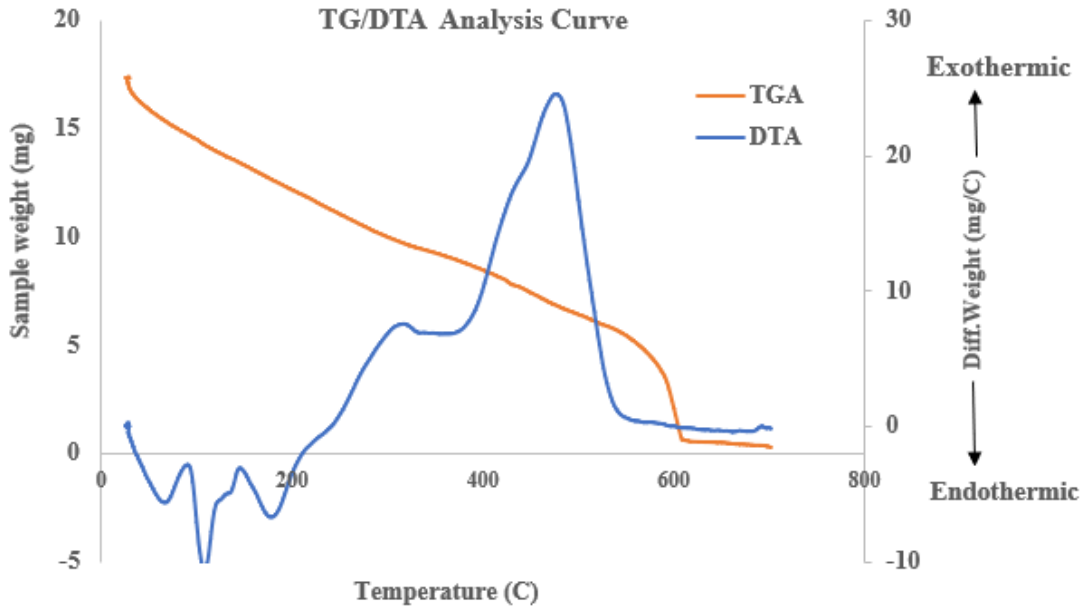

Figure 10: TG/DTA curves of cellulose-based aerogel

It is observed on the TGA curve that 8% weight loss was observed initially at temperature range between 24 ^{o}C to 55 ^{o}C. From then on it continued until 470 ^{o}C and lost 55 %. Then until it reached 610 ^{o}C the major degradation was observed losing weight by 80 %. From 620 ^{o}C on the weight was constant. From

the TGA curve it is clear that weight loss started right away then it slowed down a little with continuous but not fast weight loss. From the DTA curve the peak point where the maximum degradation occurred was at temperature 490 ^{0}C. DTA curve shows that degradation process occurred via both endothermic and exothermic processes between 26 ^{0} C and 240 ^{0} C and from around 245 ^{0} C on respectively. The degradation at the early stages could be due to the degradation of volatile matters followed by endothermic peak around 100 ^{0} C with evaporation of moisture which could not be completely removed on drying. From the TGA and DTA curves its seen that the onset temperature where major degradation started was 470 ^{0} C and the maximum degradation temperature was around 490 ^{0} C. This peak represents exothermic reactions that degraded carbonaceous matters (anhydrocellulose) parts of the aerogel. This makes the CBA thermally stable thereby it can be applicable in environments with wide range of operating temperature. This could be result of the wide pore sizes of CBA which could be mainly influenced by the WP precursors.

4.7 Efficiency Test

4.7.1 CBA Sorption capacity Test

Sorption capacity of CBA measured for cooking oil, motor/engine oil, ethanol, and benzene was calculated using (eq. 3). Figure 12 presents CBA sorption capacity for each. The CBA recorded highest absorption capacity for cooking oil i.e. 15.74 g.g^{-1}. Whereas the sorption capacities of 13.81 g.g^{-1}, 13.19 g.g^{-1}, and 13.98 g.g^{-1} were recorded for engine/motor oil, benzene and ethanol respectively. The sorption capacity of CBA is affected by not only the property of the aerogel itself but also by the properties of the pollutant depending on density, surface tension and viscosity of pollutants. The highest sorption capacity of olive oil can be due to its high density i.e. the denser the liquid the higher the sorption capacity.

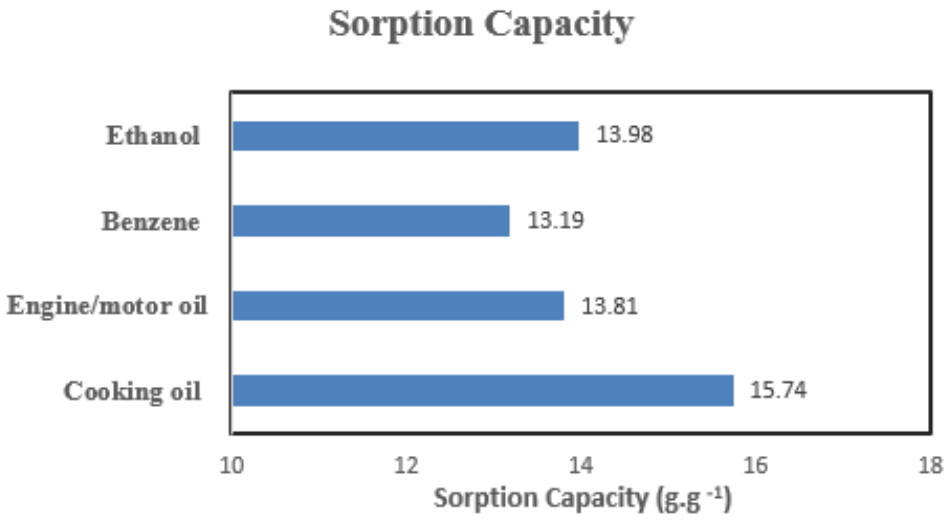

Figure 11: Sorption capacity of cellulose-based aerogel for cooking oil, motor/engine oil, ethanol, and benzene

4.7.2 Removal Efficiency Test

The removal efficiency analysis used maximum wave length of the oils/organic solvents from literature that was used on the UV/Vis spectroscopy test of contaminant liquids. The sorption capacity of CBA from the above sorption test was also used to determine the mass loading of the artificially prepared waste water. The maximum wave length, absorbed volume/mass from sorption test, viscosity, and density of each contaminant are summarized with Table 6.

Table 6: Properties and parameters of oils and organic solvents used for efficiency test (Borello & Domenici, 2019), (Nowak, Kucharska, & Kaminski, 2020).

	Cooking oil	**Engine oil**	**Ethanol (C_2H_5OH)**	**Benzene (C_6H_6)**
Density (kg/m^3)	908.7	872.5	789	876
Viscosity (Pa.sec)	74.1 x10^{-3}	228 x10^{-3}	1184.1 x10^{-6}	649 x10^{-6}
Liquid mass (g)	5.349	4.419	11.599	8.44
Volume (ml)	5.886	5.064	14.7	9.634
Max. wave length (λ_{max}) (nm)	410 nm	380 nm	210 nm	255 nm

4.7.2.1 Concentration Test for Cooking Oil

The Table 8 and Figure 19 represent the solution UV light absorbance of known concentration and the respective plot of the calibration curve, respectively, with an acceptable error range R^2 value of 0.966.CBA was used in 3 cycles and the information about its performance of removal is evaluated below. The UV/Vis test for unknown concentrations of samples, from cycle 1,2, and 3 of treated waste water were absorption values of 0.264, 0.326, and 0.392 respectively. From these concentration values the removal efficiency of CBA for food oil in each cycles are calculated using the removal efficiency equation. **:**

$$\%\ \text{Removal efficiency} = \frac{\text{Initial concentration} - \text{final concentration}}{\text{Initial concentration}} \times 100 \qquad \text{(eq. 4)}$$

The calibration equation is:

$$\mathbf{Y = 7.0703\ X + 0.1919}, \qquad \text{(eq.5)}$$

Where Y is the absorption and X is the concentration in g/ml

Cycle 1: X = (Y – 0.1919) ÷ 7.0703

X = (0.264- 0.1919) ÷ 7.0703

X = 0.0102 g/ml

Using (eq.4), the removal efficiency was calculated as;

$$\%\ \text{Removal efficiency} = \frac{0.0534 - 0.0102}{0.0534} \times 100$$

% Removal efficiency = 80.89 %

Cycle 2: X = (0.326 - 0.1919) ÷ 7.0703

X = 0.0189 g/ml

$$\%\ \text{Removal efficiency} = \frac{0.0534 - 0.0189}{0.0534} \times 100$$

% Removal efficiency = 64.6 %

Cycle 3: X = (0.350 - 0.1919) ÷ 7.0703

X = 0.0224 g/ml

$$\% \text{ Removal efficiency} = \frac{0.0534 - 0.0224}{0.0534} \text{ x } 100$$

% Removal efficiency = 58 %

4.7.2.2 Concentration Test for Engine Oil

Table 9 shows the absorbance values of known concentration that generated the standard curve shown by figure 20. The standard curve has an acceptable R^2 value of 0.986. The absorbance of waste water samples with unknown concentrations of engine oil were 0.258, 0.307, and 0.422 for cycle 1,2, and 3, respectively. From the equation, the contaminant i.e. engine oil concentration in each of the three cycles are calculated as shown below. The calibration equation here of the standard curve is;

$$\mathbf{Y = 20.461\ X + 0.051} \qquad \textbf{(}\text{eq.6)}$$

Cycle 1: From (eq.3), $X = (Y - 0.051) \div 20.461$

$X = (0.258 - 0.051) \div 20.461$

$X = 0.010$g/ml

(eq. 4) was used to calculate the removal efficiency

$$\% \text{ Removal efficiency} = \frac{0.044 - 0.0101}{0.044} \text{ x } 100 = 77.2\ \%$$

Cycle 2:

$X = (Y - 0.051) \div 20.461$

$X = (0.307 - 0.051) \div 20.461$

$X = 0.012$ g/ml

$$\% \text{ Removal efficiency} = \frac{0.044 - 0.0125}{0.044} \text{ x } 100$$

% Removal Efficiency = 71.7 %

Cycle 3: $X = (Y - 0.051) \div 20.461$

$X = (0.422 - 0.051) \div 20.461$

$X = 0.018$ g/ml

$$\% \text{ Removal efficiency} = \frac{0.044 - 0.018}{0.044} \text{ x } 100$$

% Removal Efficiency = 59.04 %

4.7.2.3 Concentration Test for Ethanol

Table 10 are the absorbance values of known ethanol concentration and Figure 21 was generated from these values. The calibration equation was extracted from the calibration curve and the correlation value (R^2) was 0.969 which is within the acceptable range. The calibration equation was;

$$\mathbf{Y = 0.4947\ X + 0.0385} \qquad \text{(eq. 7)}$$

After waste removal test using CBA, samples up to the third cycle were tested for their concentration. The tests read 0.052, 0.056, and 0.064 for the first, second and third cycles respectively. Substituting absorbance values of unknown concentration into the calibration equation the concentration values and removal efficiency were determined.

Cycle 1: From (eq.4), $X = (Y - 0.0385) \div 0.4947$

$X = (0.052 -- 0.0385) \div 0.4947$

$X = 0.0273$ g/ml

The removal efficiency was calculated using (eq.1)

$$\%\ \text{Removal efficiency} = \frac{0.116 - 0.02728}{0.116} \times 100$$

% Removal Efficiency = 76.48 %

Cycle 2: $X = (0.056 - 0.0385) \div 0.4947$

$X = 0.03537$ g/ml

$$\%\ \text{Removal Efficiency} = \frac{0.116 - 0.03537}{0.116} \times 100$$

% Removal Efficiency = 69.5 %

Cycle 3: $X = (0.064 - 0.0385) \div 0.4947$

$X = 0.05154$ g/ml

$$\%\ \text{Removal Efficiency} = \frac{0.116 - 0.05154}{0.116} \times 100$$

% Removal Efficiency = 55.5%

4.7.2.4 Concentration Test for Benzene

In a similar way as discussed above, a standard calibration curve, Figure 22, was generated using concentration and absorbance values of benzene presented by Table 11. The calibration equation with correlation factor R^2 was 0.964 was found to be;

$$\mathbf{Y = 9.2936X + 0.1419} \qquad \text{(eq. 8)}$$

The absorbance recorded was 0.345, 0.425, and 0.513 for the first, second , and third cycles respectively. From the concentration, the removal efficiency of each cycle from the initial concentration 0.0844 g/ml were found.

Cycle 1: From (eq. 8), $X = (Y - 0.141) \div 9.2936$

$X = (0.345 - 0.1419) \div 9.2936$

$X = 0.0218$ g/ml

The removal efficiency was determined using (eq.4)

$$\% \text{ Removal Efficiency} = \frac{0.0844 - 0.01173}{0.0844} \times 100$$

% Removal Efficiency = 74.1 %

Cycle 2: $X = (Y - 0.141) \div 9.2936$

$X = (0.425 - 0.141) \div 9.2936$

$X = 0.0305$ g/ml

$$\% \text{ Removal efficiency} = \frac{0.0844 - 0.0305}{0.0844} \times 100$$

$= 63.79$ %

Cycle 3: $X = (Y - 0.141) \div 9.2936$

$X = (0.513 - 0.141) \div 9.2936$

$X = 0.04$ g/ml

$$\% \text{ Removal efficiency} = \frac{0.0844 - 0.04}{0.0844} \times 100$$

% Removal Efficiency = 52.6 %

Table 7: summery of CBA removal efficiency for cooking oil, engine oil, ethanol, and benzene performed for three cycles.

Cycle No.	Removal efficiency (%)			
	Cooking oil	**Engine oil**	**Ethanol**	**Benzene**
1	80.89	77.2	76.48	74.1
2	64.6	71.7	69.5	63.79
3	58	59.04	55.5	52.6

The calculated values show sufficient removal of contaminants from waste water at the first cycle. The high tortuosity and porous nature of CBA which has low density gave CBA high buoyancy and assisted to absorb the floating oil more efficiently. The CBA showed decreasing but appreciable removal efficiency in the second and third cycles. This decreasing performance can be caused by mainly the collapse of pores and pores expanding in size that supresses the tortuous structure of fibers seen on SEM images. There is high probability for CBA to lose its hydrophobic property after every cycle due to the removal of candle soot from the CBA. The attached carbon nano particles might be lost leaving CBA to increase hydrophilicity. This decreases CBA selectivity property which affects the removal efficiency. The other factor that could cause a decrease in removal performance can be oil retention tendency of organic materials which makes the recovery of viscous oils difficult.

Chapter V

Conclusions and Recommendations

The research work aimed and successfully fabricated a biodegradable, cheap, sustainable, and efficient absorbent cellulose-based aerogel suitable for the removal of oil and organic solvents from waste water. To that end three cellulose rich organic solid waste materials were separated from solid waste stream. Waste cotton fabric, waste paper, and banana peel were selected mainly for their rich cellulose content, and used for CBA aerogel synthesis.

Sol-gel process followed by freeze drying were used to prepare a homogeneous celluloses gel and a dry, porous, and light weight cellulose-based aerogel. The CBA was synthesized varying dissolution time (1, 2, and 4 hours) and precursor/solvent ratio. The general processing of CBA was less energy intensive and environmentally safe which provides multi-faceted advantages. Pre-cooled NaOH/Urea/Water solvent system with standard ratio 7:12:81 was used to dissolve out the cellulose from precursors under continuous stirring to prepare a homogeneous sol. The other most important step was drying where freeze drying was used. It was determinant for the nature of pores i.e. pore size and distribution, in the CBA.

The final product was characterized for a number of its important properties and analysis was made. FTIR, SEM, and N_2 sorption measurement (BET surface area) were done for CBA along with evaluation of bulk density and porosity of the material. Qualitative information was extracted from FTIR spectra which shows the significant decrease of peak at 3424 cm^{-1} that indicated successful functioning of carbon nano particles to the CBA surface which can be evident that the hydrophilic property of CBA has been suppressed. The SEM images showed intertwined network of cellulose fibers which formed the complex highly porous structure of aerogel with 91.5 % of porosity. The surface area was analyzed using BET where 192 m^2/g specific surface area was obtained, which is a reasonable value that aligns with other freeze-dried CBAs. These properties of CBA make it a potential candidate for pollutant removal purposes by sorption process.

The CBA was finally used to remove oil/organic solvents from wastewater. Sorption capacities of 15.74, 13.81, 13.98, and 13.98 g/g and removal efficiency of 80.89 %, 77.2 %, 76.48 %, and 74.1 % were recorded for cooking oil, engine/motor oil, ethanol, and benzene respectively. The CBA performance as an absorbent decreased after the first cycle which can be mainly due to the collapse of pore structure. Yet the CBA removed appreciable amount of contaminant in the cycles that followed.

The research work had limitations to conduct repetitions of treatments due to a number of reasons. Mainly due to limited availability and access to laboratory resources such as freeze-dryer, and time constraint caused by laboratory shutdown during the corona pandemic restrictions. Therefore, the data provided could have statistical limitations that could lead to bias and variations in results may exist.

In conclusion, CBA was produced from abundantly available organic solid wastes which are rich in cellulose without any pretreatment. All processes were environmentally safe operations and conducted under low temperature. The recyclability, advantageous properties as an absorbent material, cheap and sustainable precursors and processing, and the reasonably appreciable removal efficiency, all make it attractive absorbent material for oil and organic solvent removal.

This particular research work could be a contribution to further studies related to combining cellulose rich materials to synthesize cellulose based aerogels. The research area could be further explored with future studies focused on:

- To start sol-gel process from recycled cellulose precursors
- To study the effect of precursor proportion specially to increase the BP proportion
- Studying the effect and performance of cellulose dissolving solvents such as ionic liquids
- To study the effect of aging time on the final cellulose-based aerogel

References

Ababa, A. (2010). Overview of Addis Ababa City Solid Waste Management SYSTEM.

Abeer, M. M., Mohd Amin, M. C. I., & Martin, C. (2014). A review of bacterial cellulose-based drug delivery systems: their biochemistry, current approaches and future prospects. Journal of Pharmacy and Pharmacology, 66(8), 1047-1061.

Aegerter, M. A., Leventis, N., & Koebel, M. (2011). Advances in sol-gel derived materials and technologies. Aerogels Handbook; Springer: New York, NY, USA.

Ali, H. M., Qasim, M. A., Malik, S., & Murtaza, G. (2018). Techniques for the Fabrication of Super-Hydrophobic Surfaces and Their Heat Transfer Applications. Heat Transfer: Models, Methods and Applications, 283.

Alireza Bazargan, J. T., and Gordon McKay. (2014). Standardization of Oil Sorbent. Journal of Testing and Evaluation.

Amera, T. (2010). Review of the Urban Environment in Ethiopia in 2008. Addis Abbeba. Ethiopian Environment Review(1).

Bayen, S. (2012). Occurrence, bioavailability and toxic effects of trace metals and organic contaminants in mangrove ecosystems: a review. Environment international, 48, 84-101.

Boinovich, L. B., & Emelyanenko, A. M. (2008). Hydrophobic materials and coatings: principles of design, properties and applications. Russian Chemical Reviews, 77(7), 583.

Borello, E., & Domenici, V. (2019). Determination of pigments in virgin and extra-virgin olive oils: A comparison between two near UV-Vis spectroscopic techniques. Foods, 8(1), 18.

Brinker, C. J., & Scherer, G. W. (1990). The physics and chemistry of sol-gel processing. Sol-Gel Science, 3, 115-119.

Cao, Y., Zhang, R., Cheng, T., Guo, J., Xian, M., & Liu, H. (2017). Imidazolium-based ionic liquids for cellulose pretreatment: recent progresses and future perspectives. Applied microbiology and biotechnology, 101(2), 521-532.

Cheru, M. (2016). Solid Waste Management in Addis Ababa: A new approach to improving the waste management system.

Cheever, M. (2011). Environmental Policy Review 2011: waste Management in Ethiopia. Environmental policy review: key issues in Ethiopia, 133.

Ciolacu, D., Rudaz, C., Vasilescu, M., & Budtova, T. (2016). Physically and chemically cross-linked cellulose cryogels: Structure, properties and application for controlled release. Carbohydrate Polymers, 151, 392-400.

Deng, X., Mammen, L., Butt, H.-J., & Vollmer, D. (2012). Candle soot as a template for a transparent robust superamphiphobic coating. Science, 335(6064), 67-70.

Dervin, S. (2017). Sol-Gel Materials for Energy, Environment and Electronic Applications, ed. SC Pillai and S. Hehir: Springer, Cham.

Dorcheh, A. S., & Abbasi, M. (2008). Silica aerogel; synthesis, properties and characterization. Journal of materials processing technology, 199(1-3), 10-26.

Dsikowitzky, L., & Schwarzbauer, J. (2013). Organic contaminants from industrial wastewaters: identification, toxicity and fate in the environment Pollutant Diseases, Remediation and Recycling (pp. 45-101): Springer.

Du, A., Zhou, B., Zhang, Z., & Shen, J. (2013). A special material or a new state of matter: a review and reconsideration of the aerogel. Materials, 6(3), 941-968.

El-Gawad, A. (2014). Oil and grease removal from industrial wastewater using new utility approach. Advances in Environmental Chemistry, 2014.

Elanthikkal, S., Gopalakrishnapanicker, U., Varghese, S., & Guthrie, J. T. (2010). Cellulose microfibres produced from banana plant wastes: Isolation and characterization. Carbohydrate Polymers, 80(3), 852-859.

Fazlollahi, F., & Wankat, P. C. (2018). Novel solvent exchange distillation column. Chemical Engineering Science, 184, 216-228.

Fricke, J., & Emmerling, A. (1992). Aerogels—Preparation, properties, applications Chemistry, Spectroscopy and Applications of Sol-Gel Glasses (pp. 37-87): Springer.

Ghasemi, M., Tsianou, M., & Alexandridis, P. (2017). Assessment of solvents for cellulose dissolution. Bioresource technology, 228, 330-338.

Gurav, J. L., Jung, I.-K., Park, H.-H., Kang, E. S., & Nadargi, D. Y. (2010). Silica aerogel: synthesis and applications. Journal of Nanomaterials, 2010.

Haile, H. (2016). Improving Solid Waste Management in Addis Ababa, Ethiopia. Based on the experience from Sweden, Östersund Municipality.

He, C., Huang, J., Li, S., Meng, K., Zhang, L., Chen, Z., & Lai, Y. (2018). Mechanically resistant and sustainable cellulose-based composite aerogels with excellent flame retardant, sound-absorption, and superantiwetting ability for advanced engineering materials. ACS Sustainable Chemistry & Engineering, 6(1), 927-936.

Heinze, T., & Koschella, A. (2005). Solvents applied in the field of cellulose chemistry: a mini review. Polímeros, 15(2), 84-90.

Henry, M. P., Donlon, B. A., Lens, P. N., & Colleran, E. M. (1996). Use of anaerobic hybrid reactors for treatment of synthetic pharmaceutical wastewaters containing organic solvents. Journal of Chemical Technology & Biotechnology: International Research in Process, Environmental AND Clean Technology, 66(3), 251-264.

Illera, D., Mesa, J., Gomez, H., & Maury, H. (2018). Cellulose Aerogels for thermal insulation in buildings: trends and challenges. Coatings, 8(10), 345.

Innerlohinger, J., Weber, H. K., & Kraft, G. (2006). Aerocellulose: aerogels and aerogel-like materials made from cellulose. Paper presented at the Macromolecular Symposia.

Jabbour, L., Gerbaldi, C., Chaussy, D., Zeno, E., Bodoardo, S., & Beneventi, D. (2010). Microfibrillated cellulose–graphite nanocomposites for highly flexible paper-like Li-ion battery electrodes. Journal of Materials Chemistry, 20(35), 7344-7347.

Jalili, V., Barkhordari, A., & Heidari, M. (2019). The role of aerogel-based sorbents in microextraction techniques. Microchemical Journal, 147, 948-954.

Jin, C., Han, S., Li, J., & Sun, Q. (2015). Fabrication of cellulose-based aerogels from waste newspaper without any pretreatment and their use for absorbents. Carbohydrate Polymers, 123, 150-156.

Jin, H., Nishiyama, Y., Wada, M., & Kuga, S. (2004). Nanofibrillar cellulose aerogels. Colloids and Surfaces A: Physicochemical and Engineering Aspects, 240(1-3), 63-67.

Khan, S. A., Khan, S. B., Khan, L. U., Farooq, A., Akhtar, K., & Asiri, A. M. (2018). Fourier transform infrared spectroscopy: fundamentals and application in functional groups and nanomaterials characterization Handbook of Materials Characterization (pp. 317-344): Springer.

Kim, C. W., Frey, M. W., Marquez, M., & Joo, Y. L. (2005). Preparation of submicron-scale, electrospun cellulose fibers via direct dissolution. Journal of Polymer Science Part B: Polymer Physics, 43(13), 1673-1683.

Kistler, S. S. (1931). Coherent expanded aerogels and jellies. Nature, 127(3211), 741-741.

Klemm, D., & Heublein, B. (2005). h.-P. Fink and A. Bohn. Angew. Chem., Int. Ed, 44, 3358-3393.

Klemm, D., Heublein, B., Fink, H. P., & Bohn, A. (2005). Cellulose: fascinating biopolymer and sustainable raw material. Angewandte chemie international edition, 44(22), 3358-3393.

Lin, X., Park, S., Choi, D., Heo, J., & Hong, J. (2019). Mechanically durable superhydrophobic PDMS-candle soot composite coatings with high biocompatibility. Journal of Industrial and Engineering Chemistry, 74, 79-85.

Liu, H., Gao, S.-W., Cai, J.-S., He, C.-L., Mao, J.-J., Zhu, T.-X., . . . Zhang, K.-Q. (2016). Recent progress in fabrication and applications of superhydrophobic coating on cellulose-based substrates. Materials, 9(3), 124.

Ma, Q., Yu, Y., Sindoro, M., Fane, A. G., Wang, R., & Zhang, H. (2017). Carbon-based functional materials derived from waste for water remediation and energy storage. Advanced materials, 29(13), 1605361.

Mäki-Arvela, P., Anugwom, I., Virtanen, P., Sjöholm, R., & Mikkola, J.-P. (2010). Dissolution of lignocellulosic materials and its constituents using ionic liquids—a review. Industrial Crops and Products, 32(3), 175-201.

Maleki, H. (2016). Recent advances in aerogels for environmental remediation applications: A review. Chemical Engineering Journal, 300, 98-118.

Maleki, H., Durães, L., & Portugal, A. (2014). An overview on silica aerogels synthesis and different mechanical reinforcing strategies. Journal of Non-Crystalline Solids, 385, 55-74.

Milazzo, G. (1981). IUPA C-Manual of Symbols and Terminology for Physico-chemical Quantities and Units| DH Whiffen (Editor). Pergamon Press, Oxford, 1979 ed., 41 pp: Elsevier.

Mitrofanov, I., Malysheva, I., Kolnoochenko, A., & Menshutina, N. (2017). Modelling of Aerogels Structures Using Intelligent System «AeroGen Structure» Computer Aided Chemical Engineering (Vol. 40, pp. 469-474): Elsevier.

Mo, J., Yang, Q., Zhang, N., Zhang, W., Zheng, Y., & Zhang, Z. (2018). A review on agro-industrial waste (AIW) derived adsorbents for water and wastewater treatment. Journal of environmental management, 227, 395-405.

Mohammed, A., & Elias, E. (2017). Domestic solid waste management and its environmental impacts in Addis Ababa city. Journal of Environment and Waste management, 4(1), 194-203.

Mohammed, M. O., Hussain, K. S., & Haj, N. Q. (2017). Preparation and bioactivity assessment of chitosan-1-acetic acid-5-flurouracil conjugates as cancer prodrugs. Molecules, 22(11), 1629.

Nguyen, S. T., Feng, J., Le, N. T., Le, A. T., Hoang, N., Tan, V. B., & Duong, H. M. (2013). Cellulose aerogel from paper waste for crude oil spill cleaning. Industrial & engineering chemistry research, 52(51), 18386-18391.

Nowak, P., Kucharska, K., & Kaminski, M. A. (2020). The New Test Procedure for Group-Type Composition of Base Oils of Lubricating Oils, Especially Emitted into the Environment. Energies, 13(15), 3772.

Nunes, L. J., Godina, R., Matias, J. C., & Catalão, J. P. (2018). Economic and environmental benefits of using textile waste for the production of thermal energy. Journal of Cleaner Production, 171, 1353-1360.

O'Connell, J. E., Saracino, P., Huppertz, T., Uniake, T., De Kruif, C. G., Kelly, A. L., & Fox, P. F. (2006). Influence of ethanol on the rennet-induced coagulation of milk. The Journal of dairy research, 73(3), 312.

Oliveira, T. Í. S., Rosa, M. F., Ridout, M. J., Cross, K., Brito, E. S., Silva, L. M., . . . Azeredo, H. M. (2017). Bionanocomposite films based on polysaccharides from banana peels. International journal of biological macromolecules, 101, 1-8.

Onwukamike, K. N., Lapuyade, L., Maillé, L., Grelier, S., Grau, E., Cramail, H., & Meier, M. A. (2019). Sustainable Approach for Cellulose Aerogel Preparation from the DBU–CO2 Switchable Solvent. ACS Sustainable Chemistry & Engineering, 7(3), 3329-3338.

Padam, B. S., Tin, H. S., Chye, F. Y., & Abdullah, M. I. (2014). Banana by-products: an under-utilized renewable food biomass with great potential. Journal of food science and technology, 51(12), 3527-3545.

Pintor, A. M., Vilar, V. J., Botelho, C. M., & Boaventura, R. A. (2016). Oil and grease removal from wastewaters: sorption treatment as an alternative to state-of-the-art technologies. A critical review. Chemical Engineering Journal, 297, 229-255.

Puneet Azad, S. R. a. R. V. (2019). Candle soot-coated egg carton material for oil water separation and detergent adsorption. Bull. Mater. Sci. Indian Academy of Sciences.

Ratke, L. (2006). Aerogels-Structure, properties and applications. Institut für Material physik im Weltraum, 51147.

RAŽIĆ, S. E., Čunko, R., Bukošek, V., & Rolich, T. (2010). Hydrophilicity improvement of cellulose-based materials by plasma. Paper presented at the Proceedings of 41 th International Symposium on Novelties in Textiles.

Riddick, J. A., Bunger, W. B., & Sakano, T. K. (1986). Organic solvents: physical properties and methods of purification.

Romelle, F. D., Rani, A., & Manohar, R. S. (2016). Chemical composition of some selected fruit peels. European Journal of Food Science and Technology, 4(4), 12-21.

Russler, A., Wieland, M., Bacher, M., Henniges, U., Miethe, P., Liebner, F., . . . Rosenau, T. (2012). AKD-Modification of bacterial cellulose aerogels in supercritical CO 2. Cellulose, 19(4), 1337-1349.

Sajjadi, S. P. (2005). Sol-gel process and its application in Nanotechnology. J. Polym. Eng. Technol, 13, 38-41.

Sandin, G., & Peters, G. M. (2018). Environmental impact of textile reuse and recycling–A review. Journal of Cleaner Production, 184, 353-365.

Sanni Babu, N., & Mutta Reddy, S. (2014). Impact of solvents leading to environmental pollution. National Seminar on Impact of Toxic Metals, Minerals and Solvents leading to Environmental Pollution. Journal of Chemical and Pharmaceutical Sciences.

Schwertfeger, F., Frank, D., & Schmidt, M. (1998). Hydrophobic waterglass based aerogels without solvent exchange or supercritical drying. Journal of Non-Crystalline Solids, 225, 24-29.

Sehaqui, H., Zhou, Q., & Berglund, L. A. (2011). High-porosity aerogels of high specific surface area prepared from nanofibrillated cellulose (NFC). Composites Science and Technology, 71(13), 1593-1599.

Sen, S., Martin, J. D., & Argyropoulos, D. S. (2013). Review of cellulose non-derivatizing solvent interactions with emphasis on activity in inorganic molten salt hydrates. ACS Sustainable Chemistry & Engineering, 1(8), 858-870.

Sing, K. S. (1985). Reporting physisorption data for gas/solid systems with special reference to the determination of surface area and porosity (Recommendations 1984). Pure and applied chemistry, 57(4), 603-619.

Singanusong, R., Tochampa, W., Kongbangkerd, T., & Sodchit, C. (2014). Extraction and properties of cellulose from banana peels. Suranaree Journal of Science and Technology, 21(3), 201-213.

Siqueira, G., Mathew, A. P., & Oksman, K. (2011). Processing of cellulose nanowhiskers/cellulose acetate butyrate nanocomposites using sol–gel process to facilitate dispersion. Composites Science and Technology, 71(16), 1886-1892.

Smirnova, I., & Gurikov, P. (2017). Aerogels in chemical engineering: Strategies toward tailor-made aerogels. Annual review of chemical and biomolecular engineering, 8, 307-334.

Smitha, S., Shajesh, P., Aravind, P., Kumar, S. R., Pillai, P. K., & Warrier, K. (2006). Effect of aging time and concentration of aging solution on the porosity characteristics of subcritically dried silica aerogels. Microporous and Mesoporous Materials, 91(1-3), 286-292.

Tewari, P. H., Hunt, A. J., & Lofftus, K. D. (1985). Ambient-temperature supercritical drying of transparent silica aerogels. Materials letters, 3(9-10), 363-367.

Thai, Q. B., Le, D. K., Luu, T. P., Do Nguyen, N. H., & Duong, H. M. Aerogels from Wastes and their Applications.

Thai, Q. B., Nguyen, S. T., Ho, D. K., Du Tran, T., Huynh, D. M., Do, N. H., . . . Phan-Thien, N. (2020). Cellulose-based aerogels from sugarcane bagasse for oil spill-cleaning and heat insulation applications. Carbohydrate Polymers, 228, 115365.

Tibolla, H., Pelissari, F. M., & Menegalli, F. C. (2014). Cellulose nanofibers produced from banana peel by chemical and enzymatic treatment. LWT-Food Science and Technology, 59(2), 1311-1318.

Torres, K., Álvarez-Hornos, F. J., San-Valero, P., Gabaldón, C., & Marzal, P. (2018). Granulation and microbial community dynamics in the chitosan-supplemented anaerobic treatment of wastewater polluted with organic solvents. Water research, 130, 376-387.

Vargas-Aponte, L. V. (2017). Evaluation of Solvents for Dissolution of Semicrystalline Cellulose. State University of New York at Buffalo.

Vargas-Jiménez, I. (2012). La entrevista en la investigación cualitativa: nuevas tendencias y retos. the interview in the qualitative research: trends and challengers. Revista Electrónica Calidad en la Educación Superior, 3(1), 119-139.

Wang, S., Lai, Z., Tran, T. H., Han, F., Su, D., Wang, R., . . . Chen, H. (2020). Solvent exchange as a synthetic handle for controlling molecular crystals. Carbon, 160, 188-195.

Xiong, B., Zhao, P., Hu, K., Zhang, L., & Cheng, G. (2014). Dissolution of cellulose in aqueous NaOH/urea solution: role of urea. Cellulose, 21(3), 1183-1192.

Xu, A., Zhang, Y., Zhao, Y., & Wang, J. (2013). Cellulose dissolution at ambient temperature: Role of preferential solvation of cations of ionic liquids by a cosolvent. Carbohydrate Polymers, 92(1), 540-544.

Yohannes, H., & Elias, E. (2017). Contamination of rivers and water reservoirs in and around Addis Ababa City and actions to combat it. Environ Pollut Climate Change, 1(116), 8.

Yu, L., Han, M., & He, F. (2017). A review of treating oily wastewater. Arabian journal of chemistry, 10, S1913-S1922.

Yuan, D., Zhang, T., Guo, Q., Qiu, F., Yang, D., & Ou, Z. (2018). Recyclable biomass carbon@ SiO2@ MnO2 aerogel with hierarchical structures for fast and selective oil-water separation. Chemical Engineering Journal, 351, 622-630.

Yue, X., Zhang, T., Yang, D., Qiu, F., & Li, Z. (2018). Hybrid aerogels derived from banana peel and waste paper for efficient oil absorption and emulsion separation. Journal of Cleaner Production, 199, 411-419.

Zanini, M., Lavoratti, A., Lazzari, L. K., Galiotto, D., Baldasso, C., & Zattera, A. J. (2018). Obtaining hydrophobic aerogels of unbleached cellulose nanofibers of the species Eucalyptus sp. and Pinus elliottii. Journal of Nanomaterials, 2018.

Zare, S., & Kargari, A. (2018). Membrane properties in membrane distillation Emerging Technologies for Sustainable Desalination Handbook (pp. 107-156): Elsevier.

Zeng, B., Wang, X., & Byrne, N. (2019). Development of cellulose-based aerogel utilizing waste denim—A Morphology study. Carbohydrate Polymers, 205, 1-7.

Zeng, B., Wang, Y., Zhang, X., & Lohse, D. (2019). Solvent Exchange in a Hele–Shaw Cell: Universality of Surface Nanodroplet Nucleation. The Journal of Physical Chemistry C, 123(9), 5571-5577.

Zhang, T., Kong, L., Dai, Y., Yue, X., Rong, J., Qiu, F., & Pan, J. (2017). Enhanced oils and organic solvents absorption by polyurethane foams composites modified with MnO2 nanowires. Chemical Engineering Journal, 309, 7-14.

Zhao, L., Zhao, K., Yan, W.-G., & Liu, Z. (2018). Preparation of assembled carbon soot films and hydrophobic properties. Materials, 11(11), 2318.

Zhou, J., & Zhang, L. (2000). Solubility of cellulose in NaOH/urea aqueous solution. Polymer Journal, 32(10), 866-870.

Zhu, L., Wang, Y., Wang, Y., You, L., Shen, X., & Li, S. (2017). An environmentally friendly carbon aerogels derived from waste pomelo peels for the removal of organic pollutants/oils. Microporous and Mesoporous Materials, 241, 285-292.

Appendix

Appendix - A

Horiba Instruments, Inc.
SA-9600 Series Surface Area Analyzer

Analysis Report
Aug/08/2020

Customer	: Kidst	Operator ID	: SARA, CHED, AASTU
Description	: Different samples :	Analysis Date	: Aug/08/2020
Filename	cellulose	Analysis Time	: 16:24:15

Condition Settings

Room Temp	: 24.0 (°C)	Atm. Pres	: 700.0 (mm)
Gas Used	: Nitrogen	Gas Conc	: 0.300, 0.002, 0.002 %

	Channel: 1	Channel: 2	Channel: 3
Sample Name	R_3t_3	R_1t_2	R_2t_2
Tube Number	1	2	3
Tare Weight	10.0160 (gm)	10.1100 (gm)	10.1330 (gm)
Sample Weight	10.0460 (gm)	10.1400 (gm)	10.1600 (gm)
Degas Temp.	120 (°C)	120 (°C)	120 (°C)
Degas Time	60 (min)	60 (min)	60 (min)
Surface Area (M^2/gm)	162.4	149.024	174.42
Slope	458.52	776.201	413.087
Intercept	-4.613	-34.73	-6.903
Vm	0.002	0.001	0.002
BET Const	-110.201	*22.052	-56.212
Pearson Coef	1.000	0.999	0.999
X[1] - 0.269	202.956	317.265	179.58
X[2] - 0.269	117.25	168.32	101.205
X[3] - 0.179	80.205	112.651	69.763

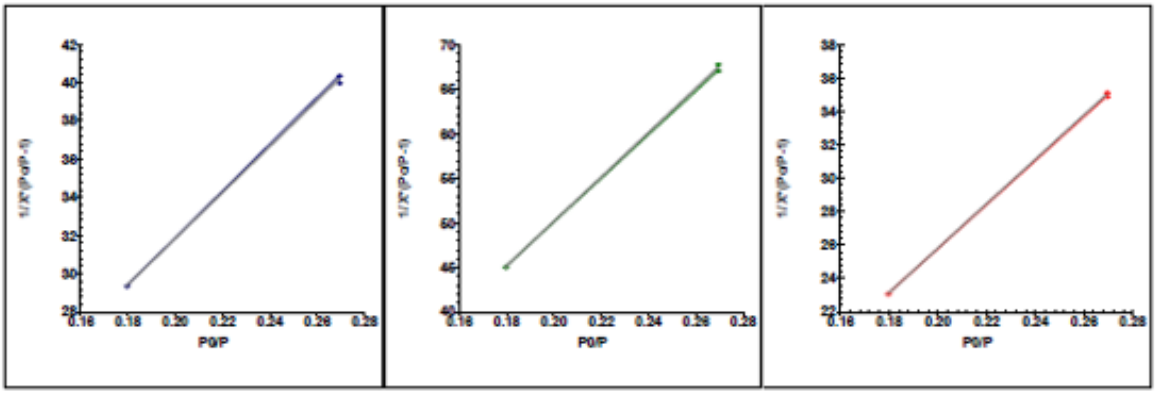

Figure 12: N_2 sorption measurement surface area analysis report for samples R_3t_3,R_1t_2, and R_2t_2

Horiba Instruments, Inc.
SA-9600 Series Surface Area Analyzer

Analysis Report
Aug/07/2020

Customer	: Kidist	Operator ID	: SARA, CHED, AASTU
Description	: Different samples :	Analysis Date	: Aug/07/2020
Filename	cellulose	Analysis Time	: 12:02:05

Condition Settings

Room Temp	: 23.0 (°C)	Atm. Pres	: 700.0 (mm)
Gas Used	: Nitrogen	Gas Conc	: 0.500, 0.002, 0.002 %

	Channel: 1	Channel: 2	Channel: 3
Sample Name	R_2t_3	R_1t_3	R_2t_1
Tube Number	1	2	3
Tare Weight	10.1340 (gm)	10.0160 (gm)	10.1170 (gm)
Sample Weight	10.1640 (gm)	10.0460 (gm)	10.0300 (gm)
Degas Temp.	200 (°C)	200 (°C)	200 (°C)
Degas Time	45 (min)	45 (min)	45 (min)
Surface Area (M^2/gm)	192.24	183.79	117
Slope	361.05	574.23	1120.801
Interoept	-17.23	-24.82	-6.892
Vm	0.003	0.0002	0.001
BET Const	-21.89	-21.021	-172.085
Pearson Coef	0.998	0.998	0.999
X[1] - 0.449	148.61	234.21	492.91
X[2] - 0.269	78.32	120.51	285.302
X[3] - 0.179	52.72	81.209	200.961

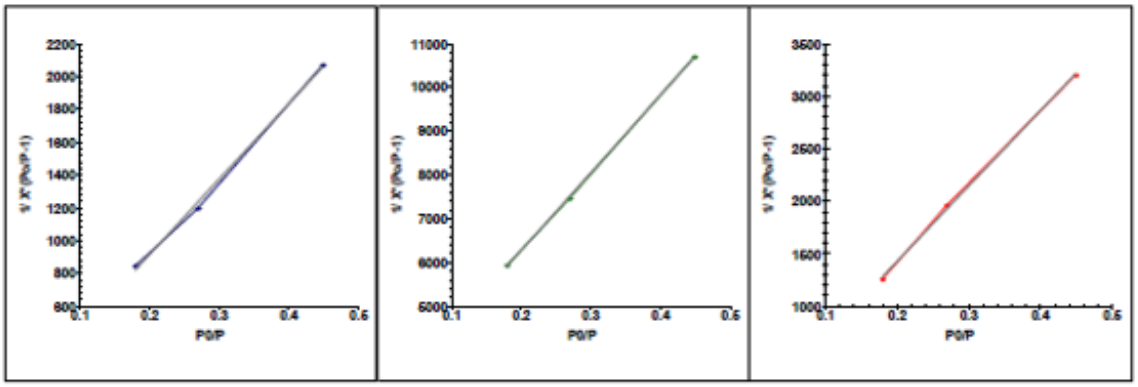

Figure 13: N_2 sorption measurement surface area analysis report for samples R_2t_3, R_1t_3, and R_2t_1

Horiba Instruments, Inc.
SA-9600 Series Surface Area Analyzer

Analysis Report
Aug/08/2020

Customer	: Kidst	Operator ID	: SARA, CHED, AASTU
Description	: Different samples :	Analysis Date	: Aug/08/2020
Filename	Cellulose	Analysis Time	: 16:24:15

Condition Settings

Room Temp	: 24.0 (°C)	Atm. Pres	: 700.0 (mm)
Gas Used	: Nitrogen	Gas Conc	: 0.300, 0.002, 0.002 %

	Channel: 1	Channel: 2	Channel: 3
Sample Name	R_1t_1	R_3t_2	R_3t_1
Tube Number	1	2	3
Tare Weight	10.0160 (gm)	10.1100 (gm)	10.1170 (gm)
Sample Weight	10.0460 (gm)	10.1400 (gm)	10.0300 (gm)
Degas Temp.	120 (°C)	120 (°C)	200 (°C)
Degas Time	60 (min)	60 (min)	45 (min)
Surface Area (M²/gm)	145.8	108.12	98.65
Slope	492.273	976.22	543.45
Interoept	-5.851	-39.89	-54.65
Vm	0.0019	0.001	0.0009
BET Const	-92.669	-26.48	-46.78
Pearson Coef	0.999	0.992	0.995
X[1] - 0.269	215.42	358.66	384.22
X[2] - 0.269	124.79	177.01	192.06
X[3] - 0.179	84.950	126.22	137.01

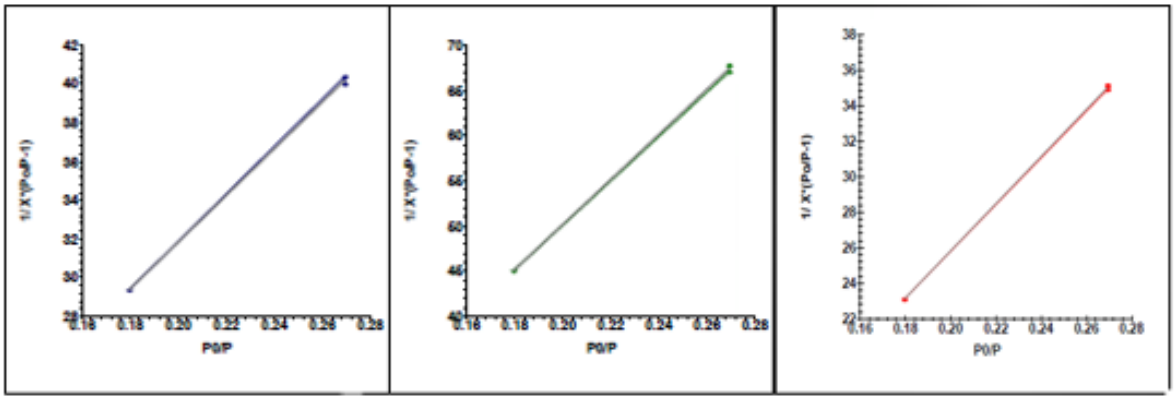

Figure 14: N_2 sorption measurement surface area analysis report for samples R_1t_1, R_3t_2, and R_3t_1

Appendix - B

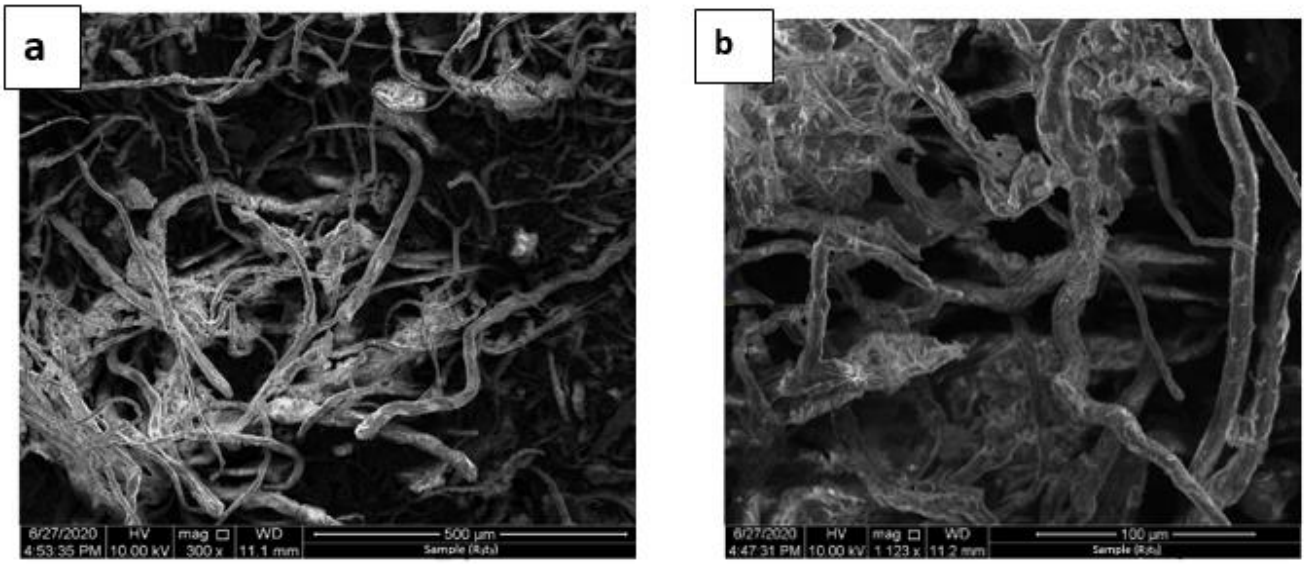

Figure 15: SEM images of samples prepared at constant ratio (R_2) and dissolution time t_1 (b), t_2 (a)

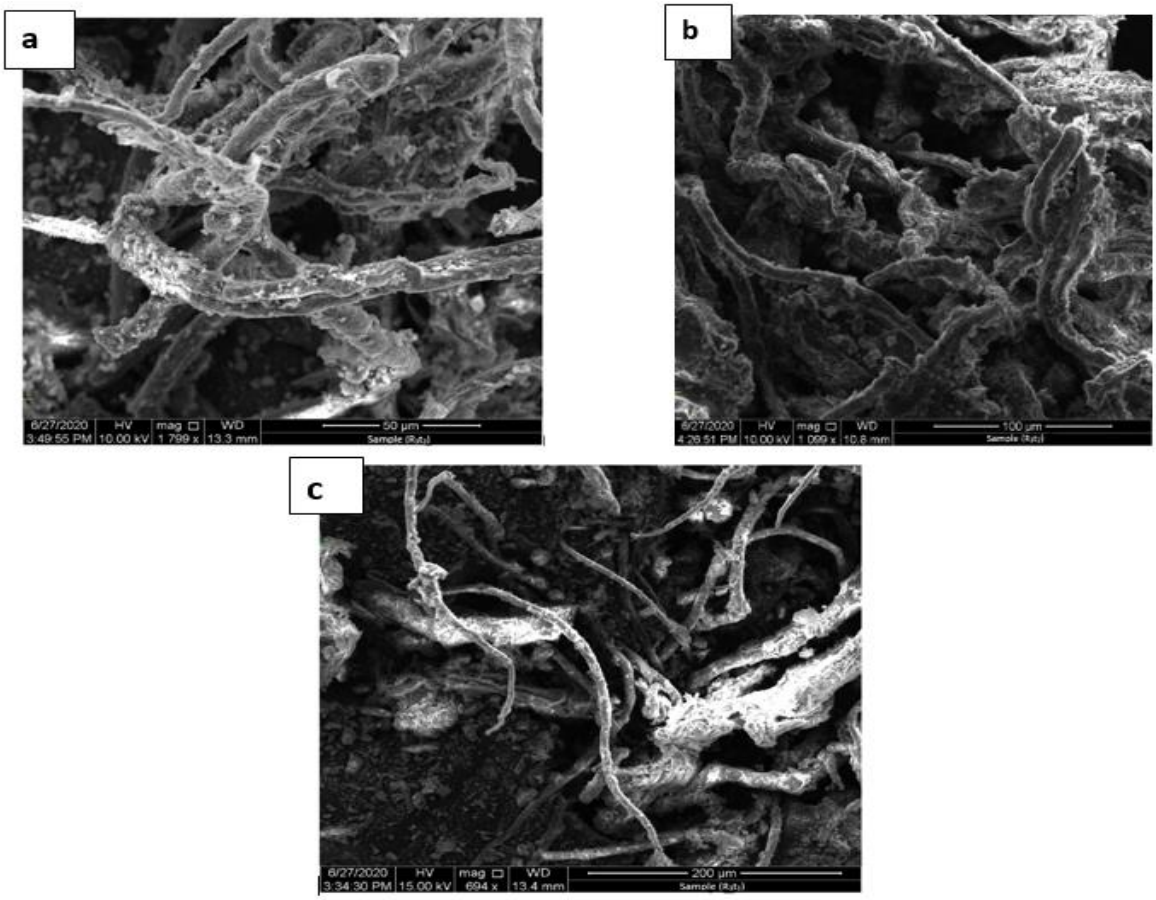

Figure 16: SEM images of samples prepared at constant ratio (R_3) and dissolution time t_1 (a), t_2 (c), and t_3 (b)

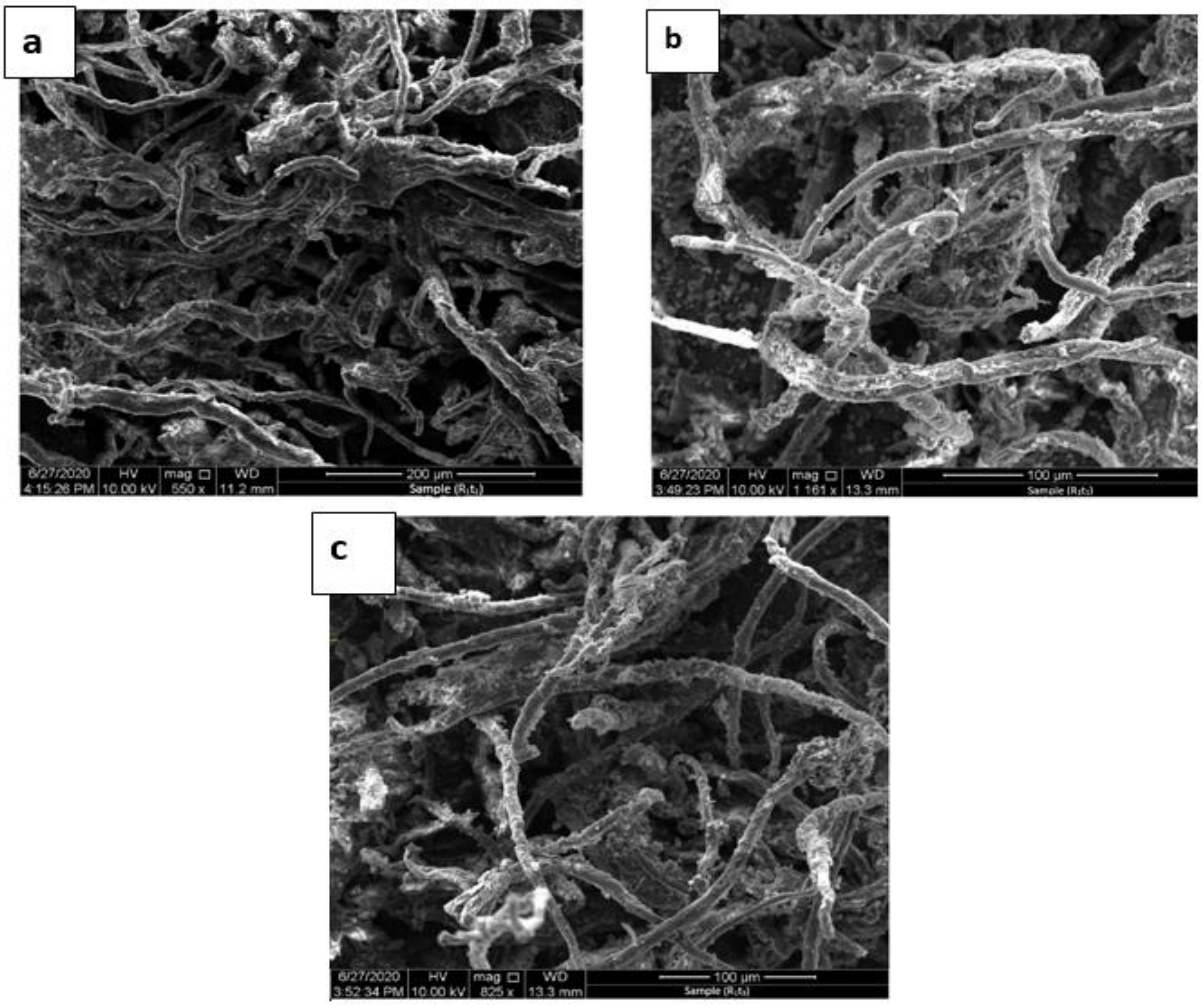

Figure 17: SEM images of samples prepared at constant ratio (R_1) and dissolution time t_1 (b), t_2 (a), and t_3 (c)

Figure 18: Test for Engine oil removal from waste water using CBA

Appendix - C

Table 8: Absorbance values of cooking oil solutions of known concentration

Concentration (g/ml)	Absorbance
0.05	0.558
0.04	0.498
0.03	0.410
0.02	0.301
0.01	0.277

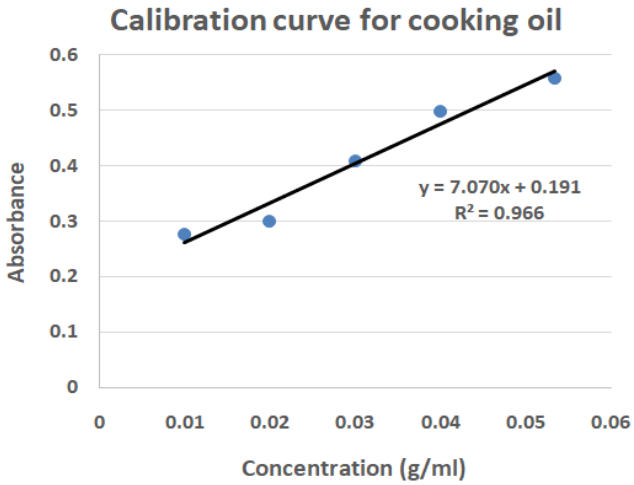

Figure 19: Calibration curve of cooking oil

Table 9: Absorbance values of engine oil solution of known concentration

Concentration (g/ml)	Absorbance
0.03	0.721
0.02	0.543
0.01	0.239
0.005	0.098

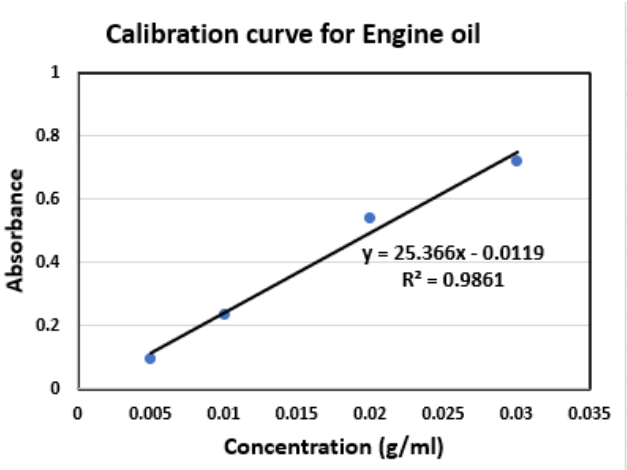

Figure 20: Calibration curve for engine oil

Table 10: Absorbance values of ethanol solutions of known concentration

Concentration (g/ml)	Absorbance
0.1	0.088
0.08	0.084
0.06	0.07
0.04	0.058
0.02	0.049

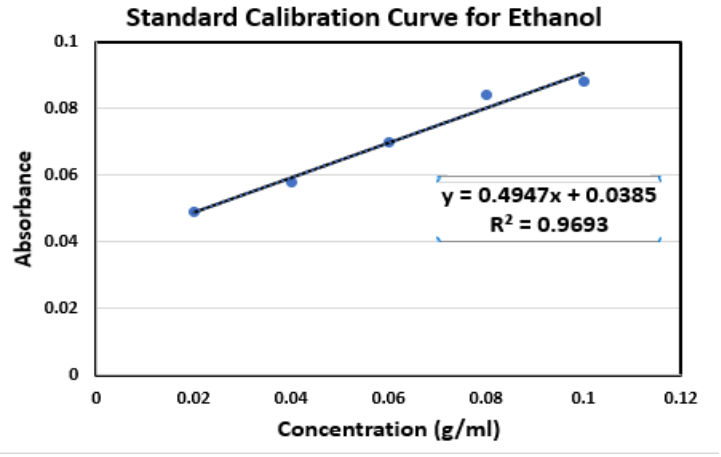

Figure 21: Calibration curve for ethanol

Table 11: Absorbance values of benzene solutions of known concentrations

Concentration (g/ml)	Absorbance
0.07	0.761
0.06	0.722
0.05	0.641
0.04	0.568
0.03	0.439

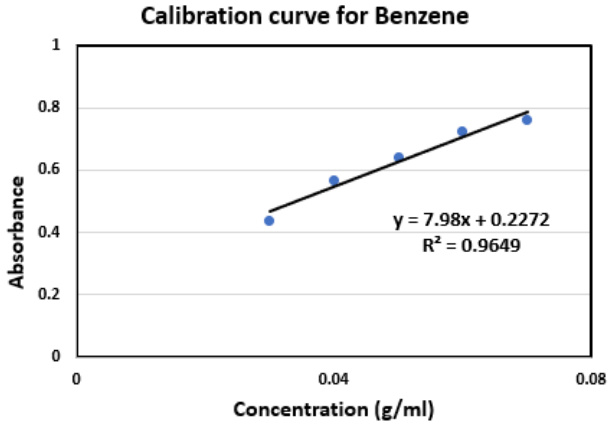

Figure 22: Calibration curve for Benzene